

CrystEngComm

Accepted Manuscript



This is an *Accepted Manuscript*, which has been through the Royal Society of Chemistry peer review process and has been accepted for publication.

Accepted Manuscripts are published online shortly after acceptance, before technical editing, formatting and proof reading. Using this free service, authors can make their results available to the community, in citable form, before we publish the edited article. We will replace this *Accepted Manuscript* with the edited and formatted *Advance Article* as soon as it is available.

You can find more information about *Accepted Manuscripts* in the [Information for Authors](#).

Please note that technical editing may introduce minor changes to the text and/or graphics, which may alter content. The journal's standard [Terms & Conditions](#) and the [Ethical guidelines](#) still apply. In no event shall the Royal Society of Chemistry be held responsible for any errors or omissions in this *Accepted Manuscript* or any consequences arising from the use of any information it contains.

Selective carbon dioxide adsorption by mixed ligand porous coordination polymers

Biswajit Bhattacharya and Debajyoti Ghoshal^{†*}



Department of Chemistry, Jadavpur University, Kolkata, 700 032, India

E-mail: dghoshal@chemistry.jdvu.ac.in

Abstract:

Porous Coordination polymers (PCPs) which are also referred as metal-organic frameworks (MOFs), have firmly established themselves as a class of excellent solid state sorbents for carbon dioxide (CO₂) along with their other several exciting properties. The mixed-ligand PCPs, constructed with polycarboxylates and N,N'-donor ligands have been adopted for the fabrication of novel functional PCPs/MOFs, as the combination of different ligands with metal ions, offer a better control over the structural variation of the frameworks compared to a single ligand. In this highlight, we have emphasized some of such important mixed linkers based MOFs with different carboxylate ligands and N,N'-donor linkers, that act as an excellent material for CO₂ adsorption, and separation. The prospect of such mixed ligand MOFs for the effective separation and sequestration of CO₂ is also addressed by means of discussing different strategies for designing mixed ligand MOFs that can potentially improve not only the amount of CO₂ adsorption, but also can increase the selectivity of CO₂ uptake over other gases and volatiles.

Authors details:

	<p>Biswajit Bhattacharya received his B.Sc. in 2007 from Vidyasagar University, India and M.Sc. in chemistry in 2009 from Rashtrasant Tukadoji Maharaj Nagpur University, India. He is currently pursuing his Ph.D in chemistry at Department of Chemistry, Jadavpur University, India, under the supervision of Dr. Debajyoti Ghoshal. His research interests are focused on mixed ligand functional coordination polymers and their applications.</p>
	<p>Debajyoti Ghoshal did his doctoral study under the guidance of Prof. N. Ray Chaudhuri at IACS and got his PhD in 2005 from Jadavpur University, India. He worked in the group of Prof. Dr. Herbert W. Roesky at University of Göttingen, Germany as an AvH fellow, to pursue his postdoctoral work. Presently he is working as a faculty in Department of Chemistry, Jadavpur University. His current research interests are crystal engineering and functional coordination polymers with a special emphasis to the selective gas storage and separation.</p>

Introduction

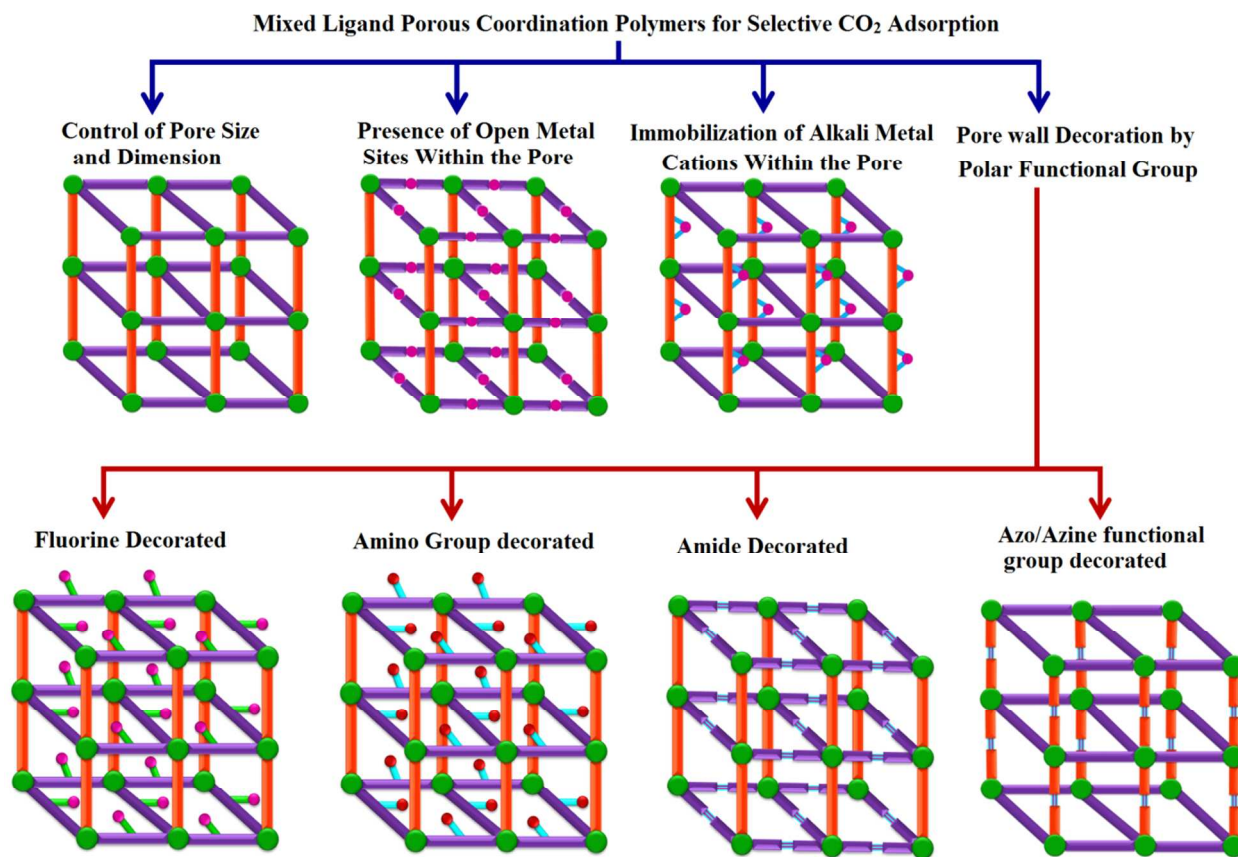
The massive emission of greenhouse gases into the atmosphere has become a significant environmental issue and it is evident from the several discussions that the carbon dioxide is the major greenhouse gas contributing to global warming causing climate change, which is one of the greatest environmental concerns facing our civilization today.¹ This alarming rise of CO₂ concentration has been originated from human activities, mainly the combustion of coal, petroleum, and natural gas which account for ~80% of CO₂ emissions worldwide, owing to economic growth and industrial development, particularly in developing countries.¹ As a result,

in recent years; there is an uncontrollable rise in the atmospheric CO₂ concentration, and that is suspected to be the principal reason behind several environmental disorders.² Presently, priority has been given by several countries to minimize the CO₂ emission, but this seems very difficult as the major source of CO₂ emission is the burning of fuels for producing energy; and civilization cannot sustain without the energy consumption. Thus, the effective control of CO₂ emission during the combustion of fossil fuel is the only possible way to save the environment. Carbon capture and sequestration (CCS) technologies that efficiently capture CO₂ from industrial flue gases could play a vital role in reducing greenhouse gas emissions. Currently, the sequestration of carbon dioxide from industrial flue gases in CCS technology, involves multiple processes including amine scrubbing and membrane separation. Amines are known to be very effective towards CO₂ capture from flue gases because of the formation of strong chemical bonds between them in the corresponding chemisorption process. But the feasible use of such amine scrubber particularly for post combustion CO₂ sequestration is not so popular, as there are huge energy involvements for the operation of such system.³ Moreover, the amine scrubbing reagents used in such processes are corrosive and unstable to heat. Amine functionalized solid absorbents such as zeolites, silicas and activated carbon based materials overcome some of the above problems to some extent, but still have some disadvantages.⁴ The pore size and pore environment of such materials are not very ordered and as a results it is very difficult to attain the selectivity in adsorption. Moreover these materials are mostly unstable in presence of water. As a matter of fact, the material may capture all components of flue gas (including N₂ which is present ~70% power plant flue gas) which will not be economically viable. Moreover, the sequestration of CO₂ in such cases sometimes requires high pressure and temperature, and sometimes the adsorption of CO₂ is irreversible.

Porous coordination polymers (PCPs), which are popularly known as metal organic frameworks (MOFs), are porous crystalline solids that are held together by coordination bonds between metal centers and organic ligands.⁵ Since their discovery, PCPs have attracted the attention of the researchers throughout the world as they have highly ordered pores, large surface areas, and high thermal stability. The advantage of PCPs with controlled pore size, shape, and functionality for specific applications is based on their design strategy which can nicely be tuned by judiciously selecting metal ions and linkers.⁶ It is worth mentioning that other factors (pH of the medium, reaction temperature, solvent, and reactant ratio) would also have an effect on the structure and

topology of the resulting frameworks.⁷ Thus the synthesis of PCPs has become a rapidly developing field over decades due to its widespread applications in various fields, such as gas storage,⁸ gas sequestration,⁹ catalysis,¹⁰ proton conductivity,¹¹ electrical conductivity,¹² and sensing¹³ etc. Using aliphatic and aromatic polycarboxylates ligands a large number of robust and/or robust/flexible PCPs or MOFs with high surface area and CO₂ adsorption capacity have been synthesized.¹⁴ But those materials can simultaneously take up significant amount of other gases also. In this context, the use of gas adsorbing MOFs, particularly which show selective CO₂ adsorption, provide for one of the most efficient approaches. Till date there has been a substantial progress in the field of CO₂ sequestration and captures by the use of PCPs or MOFs has been put forward and some excellent reviews are also done by some established groups working in this field.¹⁵ Some review work on mixed ligand MOF¹⁶ has also been done describing their structure and various functionalities. In this highlight, we will focus on the strategies for designing CO₂ adsorbing mixed ligand MOFs and the success in winning the CO₂ selectivity using such MOFs.

Certainly the use of mixed ligand MOF, for the selective CO₂ adsorption is one of the best and promising approaches. The mixed ligand MOFs are generally built by one carboxylate or other anionic linker [N_3^- , $\text{N}(\text{CN})_2^-$, PO_4^{3-} , SO_4^{2-} , SiF_6^{2-}] which brings the stability of the framework; and an organic pillar-type N,N'-donor neutral linker which give the ease of decorating the pore wall.¹⁷ In a one-liner it can be said that in the mixed ligand MOFs, the creation of design and achievement of stability can be done in one shot. In case of MOFs with mixed linkers; the dimensionality, pore size and surface area can be modulated by changing the linker size and geometry.¹⁸ Tuning of micropores of MOFs is very crucial to achieve selective gas adsorption by molecular sieving effect. Moreover, compared with single ligand based MOFs, mixed ligand MOFs allow much more flexibility in the design of the chemical environment of the pore surface by introducing different functional groups such as NH₂, OH, F, NO₂ and SO₃H. These polar substituent groups on the pore surfaces of the microporous MOF are very important to increase the CO₂-framework affinity and enforce the highly selective separation of CO₂ from the mixtures gas.¹⁹ In the light of the above point of view, it is evident that presence of pore volume alone cannot assure selective CO₂ adsorption. In fact it is a combination of proper pore size and design of the chemical environment of the pore that invariably dictates the selectivity of gas adsorption; and which can be done in an excellent way with mixed ligand PCPs.



Recently, many groups including ours has been engaged in the synthesis of mixed ligand MOFs based on polycarboxylates (aliphatic/aromatic) and N,N'-donor spacers with different metal ions for selective CO₂ adsorption.^{18d, 19i-1} In this highlight, we therefore focused on the different aspects and fine-tuning (Scheme 1) of mixed ligand PCPs structures *via* the design strategy of network for selective CO₂ adsorption. Here we are going to highlight not only on our own work in this line of enquiry but also the significant contribution made by others within the context of similar framework systems.

Discussion on design strategy for the CO₂ adsorbing MOFs

It has been already discussed that the CO₂ adsorptions by the MOF depends not only on the pore size of the MOF but also their pore environment.^{19g-h} Thus to understand the technique and strategy for achieving CO₂ adsorption and their selectivity we have discussed the issue in different broad sections along with some examples.

1. Control of pore size and dimension

Like any other gas adsorption by MOF, the adsorption of CO₂ is also dependent on the pore size and pore aperture present in the MOF. It is evident on many reports that if the pore size of any MOF is commensurate with the kinetic diameters of the particular gas then the adsorption of that gas molecule is very much feasible.¹⁸ But N₂ and CO₂ has very close kinetic diameter and that is why it is very difficult to achieve the selectivity of CO₂ over N₂ only by the fine control of the pore aperture. However there are very few reports on the selectivity by the control of pore size only, but in most of the cases the selectivity is wined by the combining the size as well as the environment. A careful design of a porous structure along with some polar group shows some adsorbent-adsorbate interactions present with the polar surface of the linker (ligand) used, and the quadruple moment of CO₂ which is absent in case of inert N₂. In such system there might be possibility of intruding N₂ within the structure, but in most of the cases the existence of unidirectional channel block the further entry of N₂ molecule making the pore inert towards N₂. Whereas in same systems the CO₂ is absorbed measurably, due to the said adsorbent-adsorbate interactions that facilitates the further adsorption of CO₂. Thus if a polar surface is present on the linkers then there is a linear relationship between the size of the pore and ease of CO₂ uptake by the MOF. This combined effect is easy to create in the resulting structure of mixed ligand MOF and have several examples of such kind, for selective CO₂ adsorption by such MOFs. In this section we are going to discuss some example where the size matters for the selectivity.

An excellent example of the design of suitable physical pore has been reported by Chen *et al* where three pillared layer frameworks are presented. The frameworks consisting of 2D square grid nets of Cu₂(CO₂)₄ with fumarate, which are linked by three organic linker pyrazine (Pyz), 4,4-bipyridine (4,4'-Bipy), and trans-bis(4-pyridyl)-ethylene (4,4'-Bpe) of different length forming doubly interpenetrated primitive cubic frameworks; {Cu(FMA)(Pyz)_{0.5}}, {Cu(FMA)(4,4'-bpy)_{0.5}·0.25H₂O} and {Cu(FMA)(4,4'-bpe)_{0.5}·0.5H₂O} (FMA = fumarate) (Fig. 1a-h).²⁰ By increasing the pillar linker length, void spaces in resultant frameworks have been rationally and steadily changed having different pore aperture of 1.4×1.8 Å² (Fig. 1d) and 2.0×3.2 Å² (Fig. 1h). The dehydrated framework of {Cu(FMA)(4,4'-bpy)_{0.5}·0.25H₂O} does not take up N₂, CH₄ and CO₂ due to the small pore size that prohibits the entry of gas molecules

(Fig. 1i). But the ultramicropores of dehydrated form of $\{\text{Cu}(\text{FMA})(4,4'\text{-bpe})_{0.5}\cdot 0.5\text{H}_2\text{O}\}$ exhibits selective sorption of CO_2 (3.3 Å) over N_2 (3.6 Å) and CH_4 (3.8 Å) at 195 K (Fig. 1i).

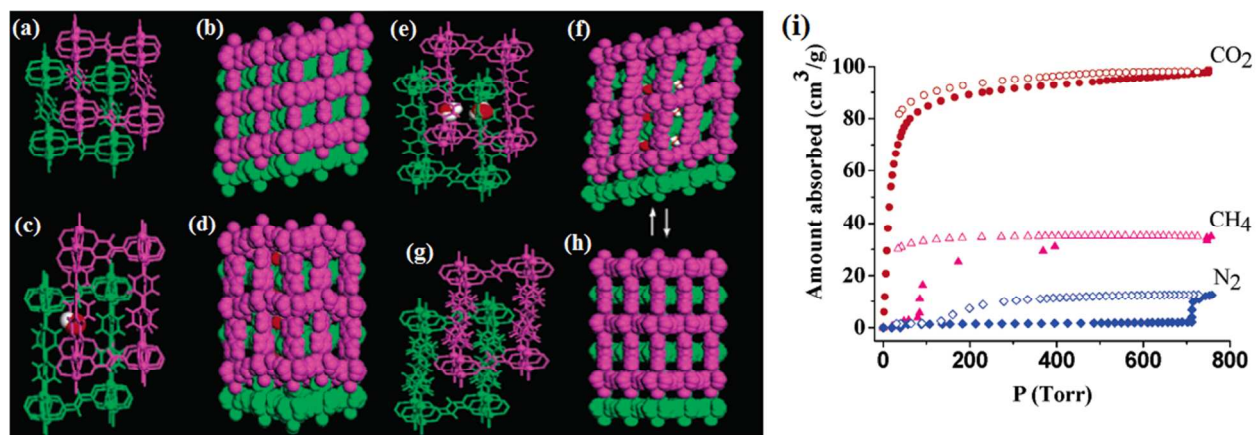


Fig. 1 Crystal structures of frameworks $\{\text{Cu}(\text{FMA})(\text{Pyz})_{0.5}\}$ (a, b), $\{\text{Cu}(\text{FMA})(4,4'\text{-bpy})_{0.5}\cdot 0.25\text{H}_2\text{O}\}$ (c, d), $\{\text{Cu}(\text{FMA})(4,4'\text{-bpe})_{0.5}\cdot 0.5\text{H}_2\text{O}\}$ (e, f), and $\{\text{Cu}(\text{FMA})(4,4'\text{-bpe})_{0.5}\}$ (g, h) showing doubly interpenetrated primitive cubic nets and corresponding pore void spaces (Cu, ball; O, red; H, white); (i) gas sorption isotherms of $\{\text{Cu}(\text{FMA})(4,4'\text{-bpe})_{0.5}\}$ at 195 K (CO_2 , red; CH_4 , pink; N_2 , blue). Reproduced with permission from ref. 20. Copyright© 2007, American Chemical Society.

Zaworotko and coworkers have also established the CO_2 selectivity by critically controlling the pore size. The resulting cubic-topology of porous materials obtained by exploring reticular chemistry approach; demonstrates exceptional selectivity, recyclability and moisture stability which are very much important in the context of CO_2 separation applications from industrial flue gas. They have reported high selectivity for the adsorption of CO_2 over N_2 and CH_4 of two MOFs, $\{[\text{Cu}(\text{bpy-1})_2(\text{SiF}_6)]\}_n$ and $\{[\text{Cu}(\text{bpy-2})_2(\text{SiF}_6)]\}_n$ [bpy-1 = 4,4'-bipyridine; bpy-2 = 1,2-bis(4-pyridyl)ethene].²¹ Structure determination revealed that the 2D grid of $\{\text{Cu}(\text{bpy-n})_2\}$ pillared by $-\text{SiF}_6^{2-}$ anionic linker resulted in a 3D framework. The effective pore size considering the van der Waals radii of the framework atoms are *ca.* 8 and 10.6 Å, respectively. However, surface area of $\{[\text{Cu}(\text{bpy-2})_2(\text{SiF}_6)]\}_n$ is almost double that of $[\text{Cu}(\text{bpy-1})_2(\text{SiF}_6)]_n$, but CO_2 uptake (12.1 wt %) of $[\text{Cu}(\text{bpy-2})_2(\text{SiF}_6)]_n$ at 298 K temperature and 1 atm pressure was found to be approximately half of that of $[\text{Cu}(\text{bpy-1})_2(\text{SiF}_6)]$ (23.1 wt %). Couple of years back, they again reported two new analogous pillared layer $-\text{SiF}_6$ functionalized frameworks by using 4,4'-dipyridylacetylene (dpa) ligand; SIFSIX-2-Cu; $[\text{Cu}(\text{dpa})_2(\text{SiF}_6)]_n$ and polymorph, SIFSIX-2-Cu-i. SIFSIX-2-Cu forms exhibits primitive-cubic net with square channels of pore dimensions

13.05 Å and polymorph phase, SIFSIX-2-Cu-i is composed of doubly interpenetrated nets that are isostructural to the nets in SIFSIX-2-Cu (Fig. 2a-b).²² Interpenetrated phase (SIFSIX-2-Cu-i)

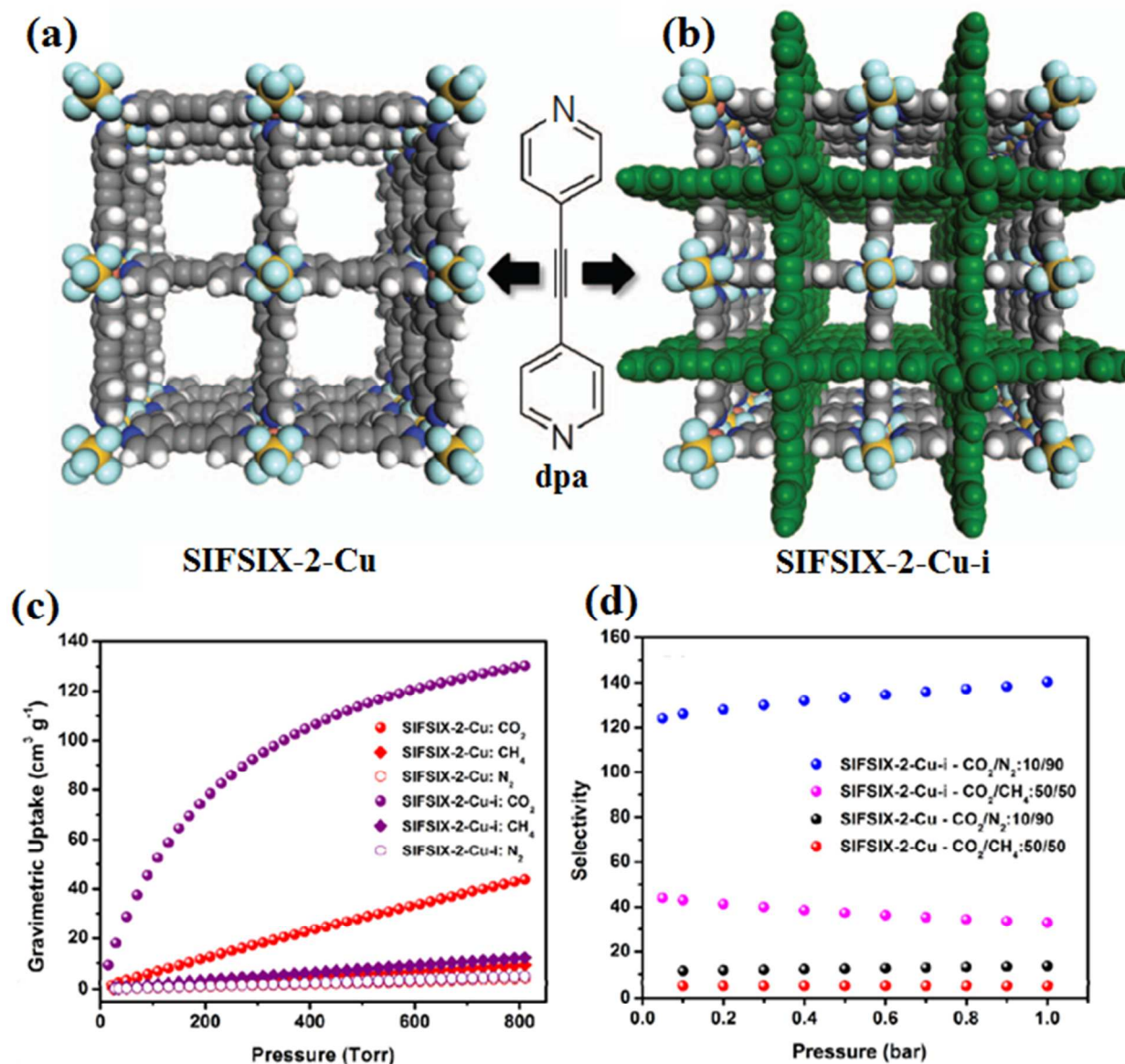


Fig. 2 The variable pore size channel structures of SIFSIX-2-Cu and SIFSIX-2-Cu-i: (a) SIFSIX-2-Cu: pore size 13.05 Å; (b) SIFSIX-2-Cu-i: pore size 5.15 Å; (c) low pressure isotherms at 298 K for SIFSIX-2-Cu (red) and SIFSIX-2-Cu-i (purple); (d) IAST selectivity of SIFSIX-2-Cu and SIFSIX-2-Cu-i, calculated from the low pressure isotherms at 298 K [CO_2/N_2 (10/90 mixture) and CO_2/CH_4 (50/50 mixture)]. Reprinted by permission from Macmillan Publishers Ltd: Nature, ref. 22. Copyright[©] 2013.

has less void space and pore window dimension than non interpenetrated phase, but the CO₂ uptake amount at 298 K and 1 atm pressure for non interpenetrated and interpenetrated variety are 41.4 and 121.2 mL g⁻¹, respectively (Fig. 2c). IAST calculations show binary gas adsorption selectivity to be significantly higher for SIFSIX-2-Cu-i than SIFSIX-2-Cu for both CO₂/CH₄ (33 versus 5.3) and CO₂/N₂ (140 versus 13.7) (Fig. 2d). It is interesting to note that, CO₂ uptake of SIFSIX-2-Cu-i at 298K and 1 bar is among the highest so far reported in the context of MOFs which established the accomplishment by the proper design.

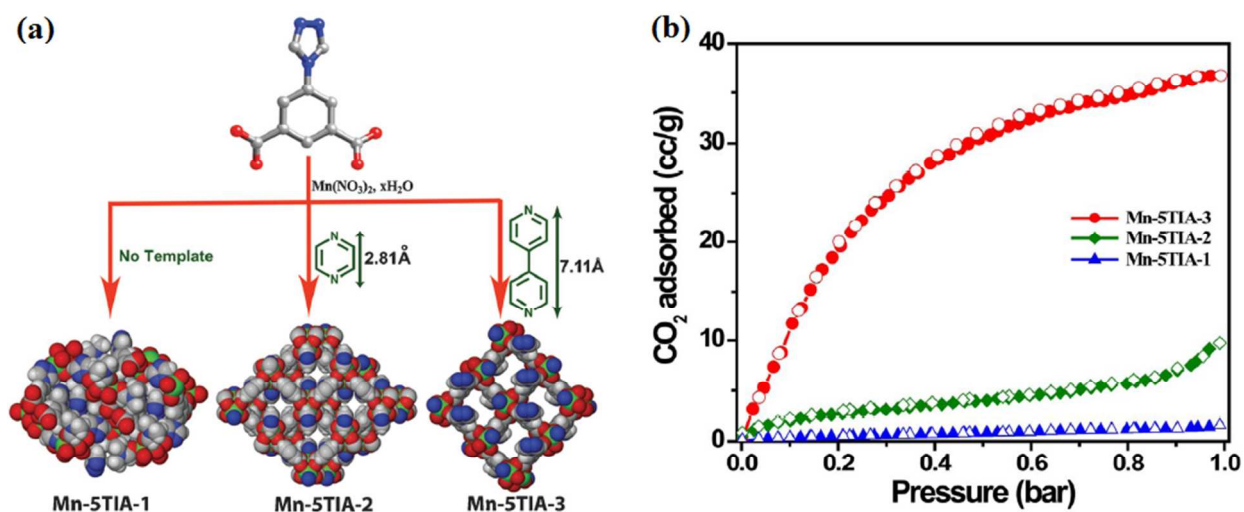


Fig. 3 (a) Synthesis of Mn-MOFs showing enhancement of porosity depending on the size of templates used during synthesis; (b) the CO₂ gas-sorption isotherms for Mn-5TIA-1 -2 and -3 measured at 298 K (The filled and open circles represent adsorption and desorption branches, respectively). Reproduced from ref. 23.

Examples are also there where CO₂ selectivity is observed by controlling both size and environment too. An appealing example by Banerjee *et al* shows a measurable enhancement of porosity and formation of nonporous to microporous isomeric MOFs from the same reactants by increasing the size of the template for selective CO₂ adsorption over N₂ and CH₄ (Fig. 3a). They synthesized three isomeric MOFs; Mn-5TIA-1, Mn-5TIA-2 and Mn-5TIA-3 using 5-triazole isophthalic acid (5-TIA).²³ Mn-5TIA-1 is a 3D nonporous net which was prepared without any linker template. Mn-5TIA-2 and Mn-5TIA-3 were synthesized using pyrazine or 4,4'-bipy, respectively, as linkers and resulted in formation of cross linked square grid nets in both the

cases having pore apertures of $\sim 2.57 \text{ \AA}$ and $\sim 7.22 \text{ \AA}$, respectively (Fig. 3a). The pore apertures of Mn-5TIA-2 and Mn-5TIA-3 are comparable to the length of the pyrazine and 4,4'-bipy linkers. All three frameworks does not uptake any N_2 at 77 K but shows an increasing CO_2 uptake in Mn-5TIA-1, Mn-5TIA-2 and Mn-5TIA-3 of 2 cc gm^{-1} , 9.85 cc gm^{-1} and 37.45 cc gm^{-1} respectively at 298 K which is very much commensurate with the pore size of these frameworks (Fig. 3b).

In this context, recently our group has reported three 3D MOFs of succinate dianion, with the combination of three different pyridyl-based linkers.²⁴ In all three compounds $\{[\text{Cd}(\text{L1})(\text{suc})] \cdot (\text{H}_2\text{O})_3\}_n$, $\{[\text{Cd}(\text{L2})(\text{suc})] \cdot (\text{H}_2\text{O})_2\}_n$ and $\{[\text{Cd}(\text{L3})(\text{suc})] \cdot (\text{H}_2\text{O})_4\}_n$; [suc = succinate dianion, L1 = 2,5-Bis-(4-pyridyl)-3,4-diaza-2,4-hexadiene, L2 = trans 4,4'-azobispyridine and L3 = 2,5-bis-(3-pyridyl)-3,4-diaza-2,4-hexadiene] the succinate dianions connect to metal centers creating two-dimensional metal carboxylate moieties, which are then pillared by pyridyl-based linkers forming three dimensional frameworks (Fig. 4a-c). In case of $\{[\text{Cd}(\text{L1})(\text{suc})] \cdot (\text{H}_2\text{O})_3\}_n$ and $\{[\text{Cd}(\text{L2})(\text{suc})] \cdot (\text{H}_2\text{O})_2\}_n$, the linkers L1 and L2 are different in terms of length but both the linkers have the pyridyl-N at the 4-position of the pyridine ring (Fig. 4a-b). This results in a formation of regular water filled channels within the framework structures in these two cases (Fig. 4d-e), whereas in the case of $\{[\text{Cd}(\text{L3})(\text{suc})] \cdot (\text{H}_2\text{O})_4\}_n$ the positional change (4 to 3) of the pyridyl-N atom in L3 makes it bent, which leads to the partial blockage of regular channels in $\{[\text{Cd}(\text{L3})(\text{suc})] \cdot (\text{H}_2\text{O})_4\}_n$ (Fig. 4f). The channel dimensions of $\{[\text{Cd}(\text{L1})(\text{suc})] \cdot (\text{H}_2\text{O})_3\}_n$ is higher than $\{[\text{Cd}(\text{L2})(\text{suc})] \cdot (\text{H}_2\text{O})_2\}_n$ due to the difference in length of the linkers. All three frameworks does not show any N_2 uptake but $\{[\text{Cd}(\text{L1})(\text{suc})] \cdot (\text{H}_2\text{O})_3\}_n$ and $\{[\text{Cd}(\text{L2})(\text{suc})] \cdot (\text{H}_2\text{O})_2\}_n$, at 273 K show reversible uptake of 5.86 and 4.47 wt % of CO_2 respectively, as the pressure approaches to 1 atm (Fig. 4g). Due to the use of bent linker L3 in $\{[\text{Cd}(\text{L3})(\text{suc})] \cdot (\text{H}_2\text{O})_4\}_n$, the pore dimension is reduced, and as a result almost no gas adsorption is observed in case of dehydrated framework of $\{[\text{Cd}(\text{L3})(\text{suc})] \cdot (\text{H}_2\text{O})_4\}_n$ (Fig. 4h).

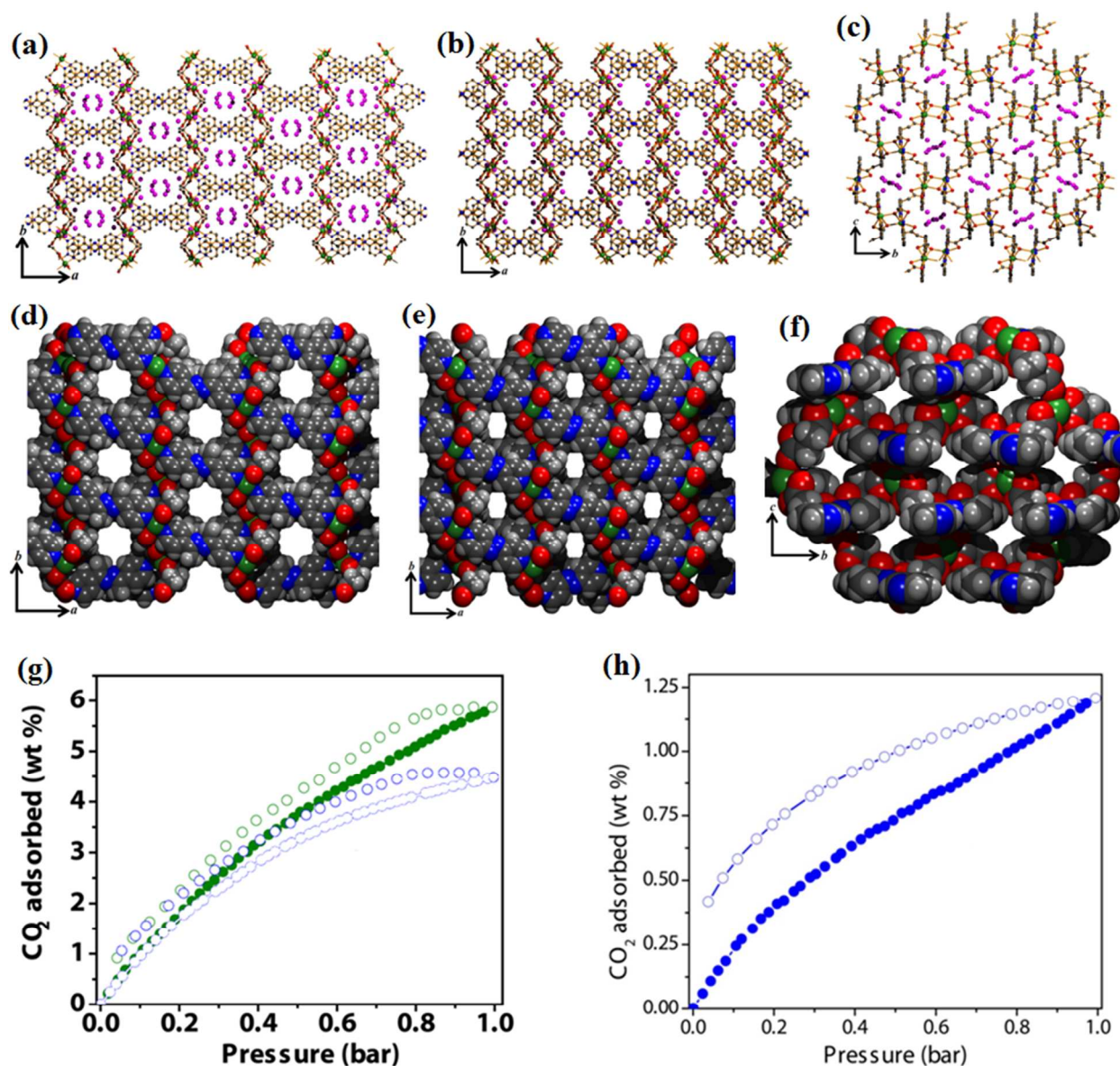


Fig. 4 (a, b, c) 3D structure with water filled 1D channels in $\{[\text{Cd}(\text{L1})(\text{suc})] \cdot (\text{H}_2\text{O})_3\}_n$, $\{[\text{Cd}(\text{L2})(\text{suc})] \cdot (\text{H}_2\text{O})_2\}_n$ and $\{[\text{Cd}(\text{L3})(\text{suc})] \cdot (\text{H}_2\text{O})_4\}_n$; (d, e, f) the space filling models of dehydrated frameworks showing the 3D empty channels of $\{[\text{Cd}(\text{L1})(\text{suc})] \cdot (\text{H}_2\text{O})_3\}_n$, $\{[\text{Cd}(\text{L2})(\text{suc})] \cdot (\text{H}_2\text{O})_2\}_n$ and $\{[\text{Cd}(\text{L3})(\text{suc})] \cdot (\text{H}_2\text{O})_4\}_n$; (g) CO_2 adsorption isotherms for $\{[\text{Cd}(\text{L1})(\text{suc})]\}_n$ (green) and $\{[\text{Cd}(\text{L2})(\text{suc})]_2\}_n$ (blue) at 273 K temperature; (h) CO_2 adsorption isotherms for $\{[\text{Cd}(\text{L3})(\text{suc})]\}_n$ (filled and open circles represent adsorption and desorption respectively). Reproduced with permission from ref. 24. Copyright[©] 2013, American Chemical Society.

2. Presence of open metal sites within the pore

One of the promising techniques for preparing the gas adsorbing MOF is the creation of unsaturated metal centers in the coordination space which is also known as open metal sites. These open metal sites can feebly interact with the incoming gas molecules, resulting better affinity of gas molecules with the MOF.²⁵ Carbon dioxide being a gas with quadruple moment can effectively interact with the coordinately unsaturated metal centers. The systematic immobilization of open metal sites into the mixed ligand based MOFs are quite challenging because in most cases metal atoms are coordinately saturated by organic ligands and coordinated solvent molecules. If metal coordinated volatile solvent is present in the framework, then the unsaturated metal sites can be created in the cavity of MOF, by the removal of such solvent molecules without disturbing the framework structure. This is normally done by controlled heating of the MOF, by applying vacuum or using both. Coordinatively unsaturated metal centers within porous MOFs have played significant roles in gas storage and separation particularly showing some selectivity towards CO₂. Here some of the examples of mixed ligand system have been discussed for the sake of understanding.

The use of the metalloligand building block is an approach which seems very promising for the immobilization of open metal sites into the porous mixed ligand MOFs. Kitagawa *et al.* and Chen *et al.* utilized several metalloligands to synthesize porous mixed ligand functional MOFs.²⁶⁻²⁷ By using [Cu(Pyac)₂] metalloligand, Kitagawa *et al.* reported a mixed ligand pillared-layer porous coordination polymers; [$\{\text{Cu}_2(\text{pzdc})_2\text{Cu}(\text{Pyac})_2\text{H}_2\text{O}\} \cdot 4\text{H}_2\text{O}\}_n$ (Pyac = 3-(4-pyridyl)pentane-2,4-dionato, Na₂pzdc = disodium 2,3-pyrazinedicarboxylate) having open Cu(II) center (Fig. 5a-e).²⁶ This system exhibits an interesting reversible single crystal to single crystal transformation which is triggered by the removal of a water molecule on a Cu(II) site in the pore. The desolvated framework of this compound; [$\{\text{Cu}_2(\text{pzdc})_2\text{Cu}(\text{Pyac})_2\}_n$], showed very high amount of CO₂ uptake at 195 K.

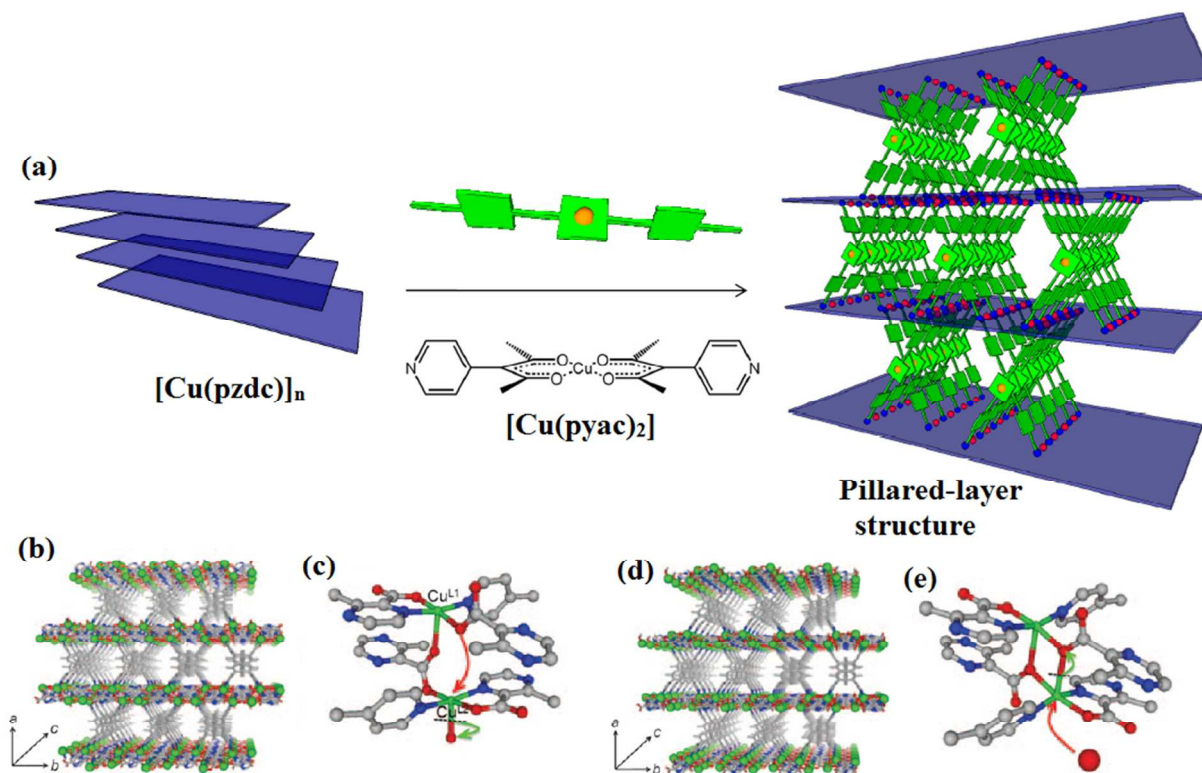


Fig. 5 (a) Schematic representations of crystal structures of a pillared-layer PCP; (b) extended structure of $[\{\text{Cu}_2(\text{pzdc})_2\text{Cu}(\text{Pyac})_2\text{H}_2\text{O}\}]_n$ viewed along the c axis (H_2O molecules are omitted); (c) local structure around Cu centers in $[\{\text{Cu}_2(\text{pzdc})_2\text{Cu}(\text{Pyac})_2\text{H}_2\text{O}\}]_n$; (d) extended structure of $[\{\text{Cu}_2(\text{pzdc})_2\text{Cu}(\text{Pyac})_2\}]_n$ viewed along the c axis; (e) local structure around $[\text{Cu}_2(\mu\text{-O})_2]$ centers in $[\{\text{Cu}_2(\text{pzdc})_2\text{Cu}(\text{Pyac})_2\}]_n$. Reproduced with permission from ref. 26. Copyright © 2009, WILEY-VCH Verlag GmbH & Co. KGaA, Weinheim.

Using the metallo-ligand approach, Chen *et al.* also synthesized a three-dimensional triply interpenetrated microporous mixed ligand MOF, $\text{Zn}_2(\text{BBA})_2(\text{CuPyen})\cdot\text{Gx}$ (BBA = biphenyl-4,4'-dicarboxylate; G = guest solvent molecules) by using salen precursor metallo-ligand $\text{Cu}(\text{PyenH}_2)(\text{NO}_3)_2$ (PyenH_2 = 5-methyl-4-oxo-1,4-dihydro-pyridine-3-carbaldehyde) (Fig. 6a-c).²⁷ This compound also contains an open $\text{Cu}(\text{II})$ site on the pore surface which influences its highly selective $\text{C}_2\text{H}_2/\text{CH}_4$ and CO_2/CH_4 gas separation at ambient temperature (Fig. 6d-e). It is worth to mention here that the presence of three fold framework interpenetration is also act additively for the aforesaid selectivity (Fig. 6d-e).

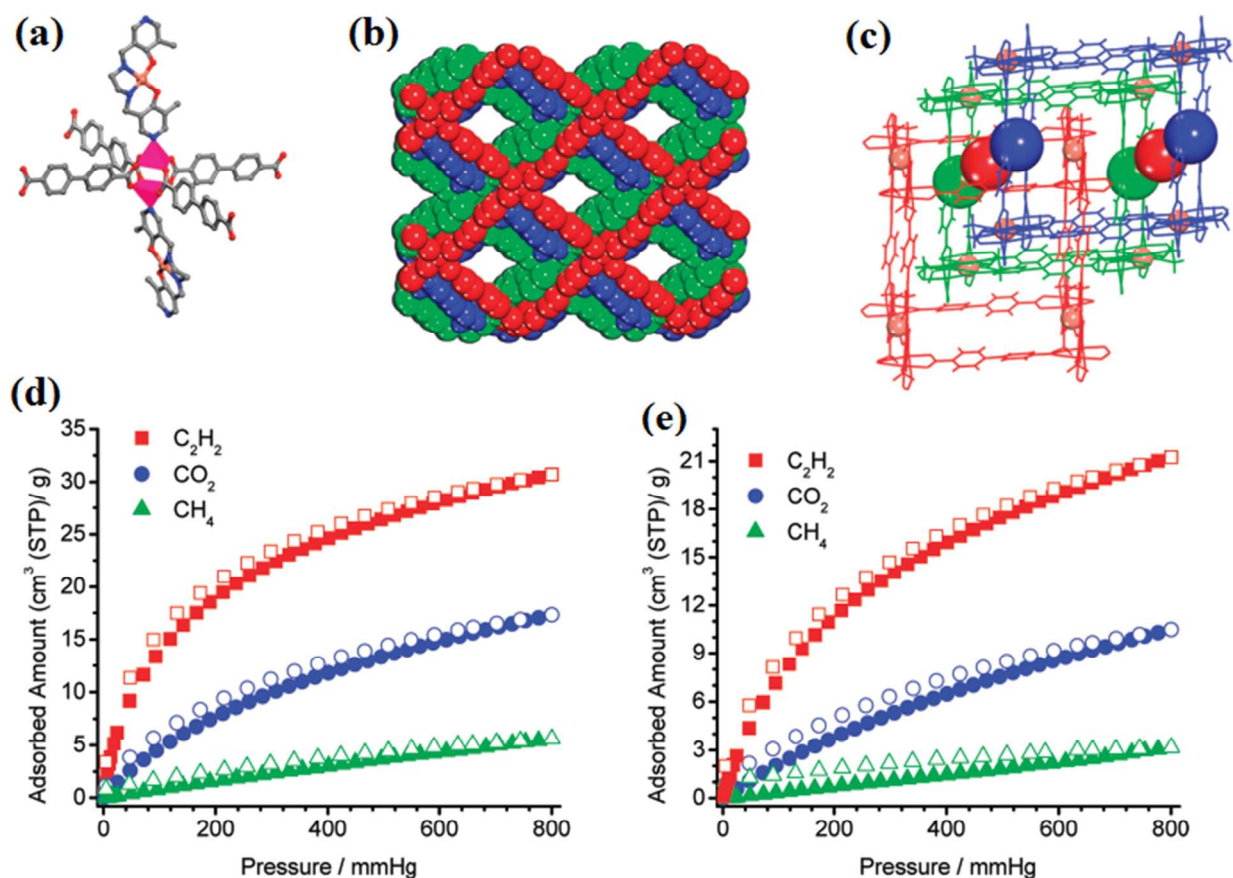


Fig. 6 Structure of $\text{Zn}_2(\text{BBA})_2(\text{CuPyen}) \cdot \text{Gx}$: (a) the paddle wheel $\{\text{Zn}_2(\text{COO})_4\}$ node linked by four BBA and two Cu(Pyen); (b) space-filling diagram showing triple interpenetration with a 1D channel along the c direction; (c) perspective views triply interpenetrated network with immobilized open Cu^{2+} sites; (d, e) adsorption (solid) and desorption (open) isotherms of acetylene (red squares), carbon dioxide (blue circles), and methane (green triangles) on $\text{Zn}_2(\text{BBA})_2(\text{CuPyen})$ at 273 K (left) and 295 K (right). Reproduced with permission from ref. 27. Copyright © 2012, American Chemical Society.

Maji *et al.* recently reported a mixed ligand based 3D porous pillared layer framework of Zn^{2+} , $\{[\text{Zn}_2(\text{H}_2\text{dht})(\text{dht})_{0.5}(\text{azpy})_{0.5}(\text{H}_2\text{O})] \cdot 4\text{H}_2\text{O}\}_n$ (H_2dht = 2,5-dihydroxyterephthalic acid and azpy = 4,4'-azobipyridine) with two different types of channels having unsaturated Zn(II) sites (after the removal of coordinated H_2O molecules) and polar $-\text{OH}$ group (Fig. 7a-b).²⁸ The dehydrated framework of this MOF shows highly selective adsorption of CO_2 (21.2 wt%) over other gases, such as N_2 , H_2 , O_2 and Ar, at 195 K with high value of isosteric heat of adsorption ($Q_{\text{st}} = 33.4 \text{ kJmol}^{-1}$) (Fig. 7c).

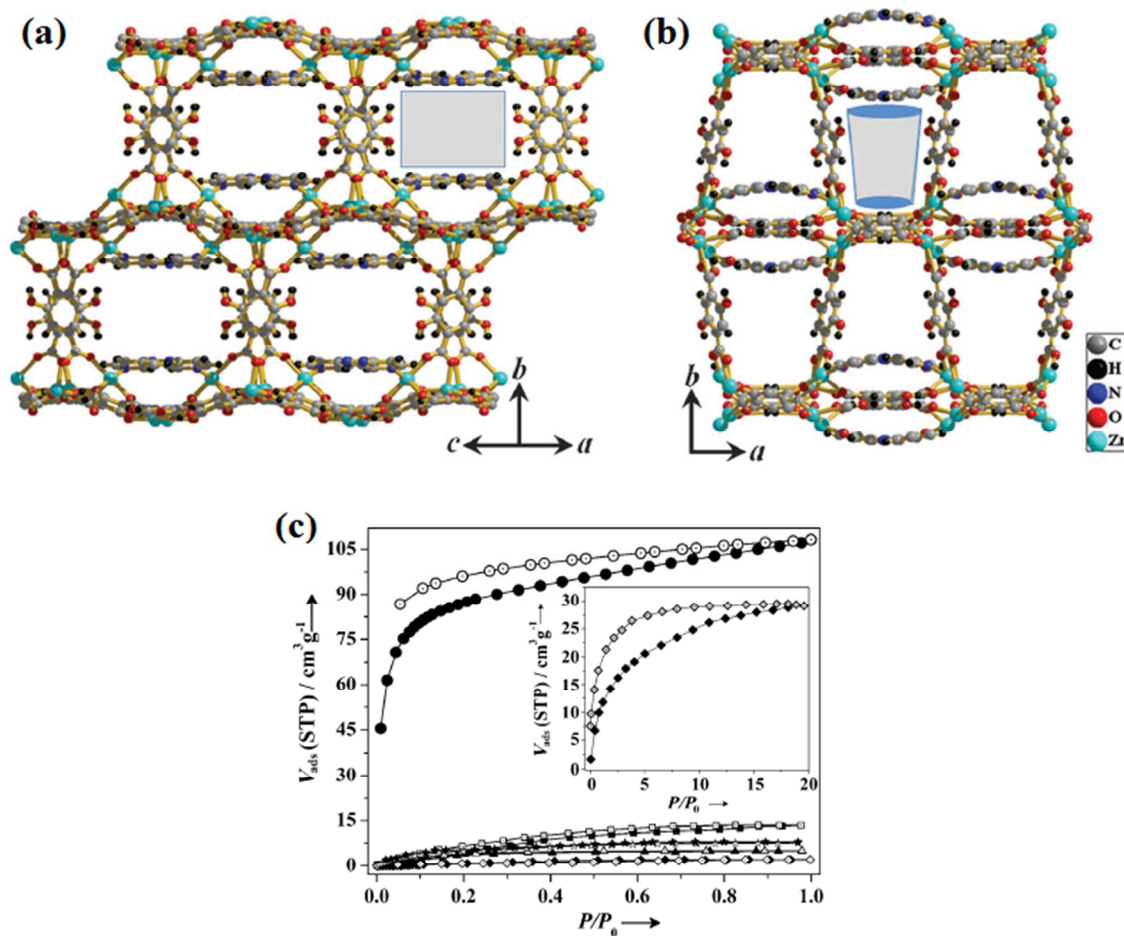


Fig. 7 (a) View of rectangle- and (b) calyx-shaped channels along the [101] and [001] directions in $\{[\text{Zn}_2(\text{H}_2\text{dht})(\text{dht})_{0.5}(\text{azpy})_{0.5}(\text{H}_2\text{O})]\cdot 4\text{H}_2\text{O}\}_n$; (c) gas adsorption isotherms for desolvated $\{[\text{Zn}_2(\text{H}_2\text{dht})(\text{dht})_{0.5}(\text{azpy})_{0.5}(\text{H}_2\text{O})]\cdot 4\text{H}_2\text{O}\}_n$; CO_2 (circles), Ar (squares), O_2 (diamonds) at 195 K, and N_2 (triangles) and H_2 (stars) at 77 K. Inset of (c) shows the CO_2 adsorption isotherm measured at 298 K and 20 bar (solid symbols indicate adsorption and open symbols indicate desorption; P_0 is the saturated vapour pressure of the adsorbates at measurement temperatures). Reproduced with permission from ref. 28. Copyright© 2012, WILEY-VCH Verlag GmbH & Co. KGaA, Weinheim.

3. Immobilization of alkali metal cations within the pore

As mentioned before the CO_2 has quadruple moment, the introduction of electropositive alkali metal into the framework structure is one of the suitable approaches to enhance the CO_2 -philicity of the framework by increasing sorbent–sorbate interactions within the MOF. Immobilization of

alkali metal into the framework is generally carried out by using alkali metal hydroxide in the reaction medium or by reduction of the framework containing redox-active ligand.

Kitagawa *et al.* reported a heterometallic PCP,²⁹ $\{[\text{CdNa}(2\text{-stp})(\text{dabco})_{0.5}(\text{H}_2\text{O})].2\text{H}_2\text{O}\}_n$ (2-stp = 2-sulfonylterephthalate, dabco = 1,4-Diazabicyclo [2,2,2]octane) which consist of 1D channels along the *b* axis with a cross-section of approximately $4.9 \times 4.9 \text{ \AA}^2$, and the sodium cations are immobilized on the pore surfaces with one coordinated water molecule (Fig. 8a-d). Thermogravimetric analysis (TGA) indicates that

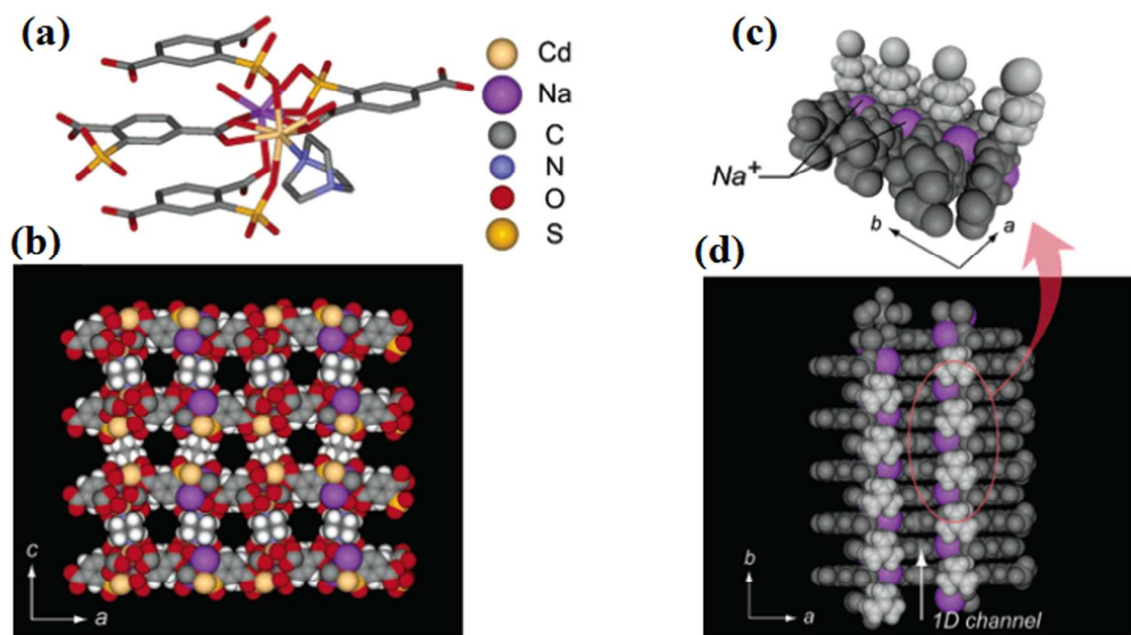


Fig. 8 (a) Crystallographic environment around Cd(II) and Na(I) centres (H atoms are omitted); (b) three-dimensional assembled structure of $\{[\text{CdNa}(2\text{-stp})(\text{dabco})_{0.5}(\text{H}_2\text{O})].2\text{H}_2\text{O}\}_n$ (guests are omitted); (c) view of the coordination environment around Na(I); (d) a cross-section of 1D channel of $\{[\text{CdNa}(2\text{-stp})(\text{dabco})_{0.5}]\}_n$ along the *b* axis (purple, dark gray, and light gray represent Na(I), 2D sheet, and pillar ligand systems, respectively). Reproduced with permission from ref. 29. Copyright[©] 2006, American Chemical Society.

the dehydrated framework $\{[\text{CdNa}(2\text{-stp})(\text{dabco})_{0.5}]\}_n$ was generated at $150 \text{ }^\circ\text{C}$ and that dehydrated framework possess pentacoordinated sodium ions with their sixth site open for a guest, which are regularly embedded in the 1D pore wall. PXRD pattern of the dehydrated framework showed similarity to that of the as-synthesized framework suggesting the same structural

topology. The microporous framework was then stable up to 330 °C. The CO₂ uptake at 195 K revealed a typical type-I curve and the saturated adsorbed amount of CO₂ is about 92.6 mL/g at $P/P_0 = 0.95$ and which is equivalent to 1.8 molecules per Na(I) ion.

It has been interesting to note that for the purpose of enhancement of selective gas adsorption; recently redox center has also been incorporated into the pore wall of mixed ligand MOF. Redox-active zinc based mixed-ligand MOFs, $\{Zn_2(ndc)_2(diPyNI)\}$ (**1**), and $\{Zn_2(TCPB)(DPG)\}$ (**2**) (ndc = 2,6-naphthalenedicarboxylate, diPyNI = N,N'-di-(4-pyridyl)-1,4,5,8-naphthalenetetracarboxy diimide; TCPB = 1,2,4,5-tetrakis(4-carboxyphenyl)-benzene)

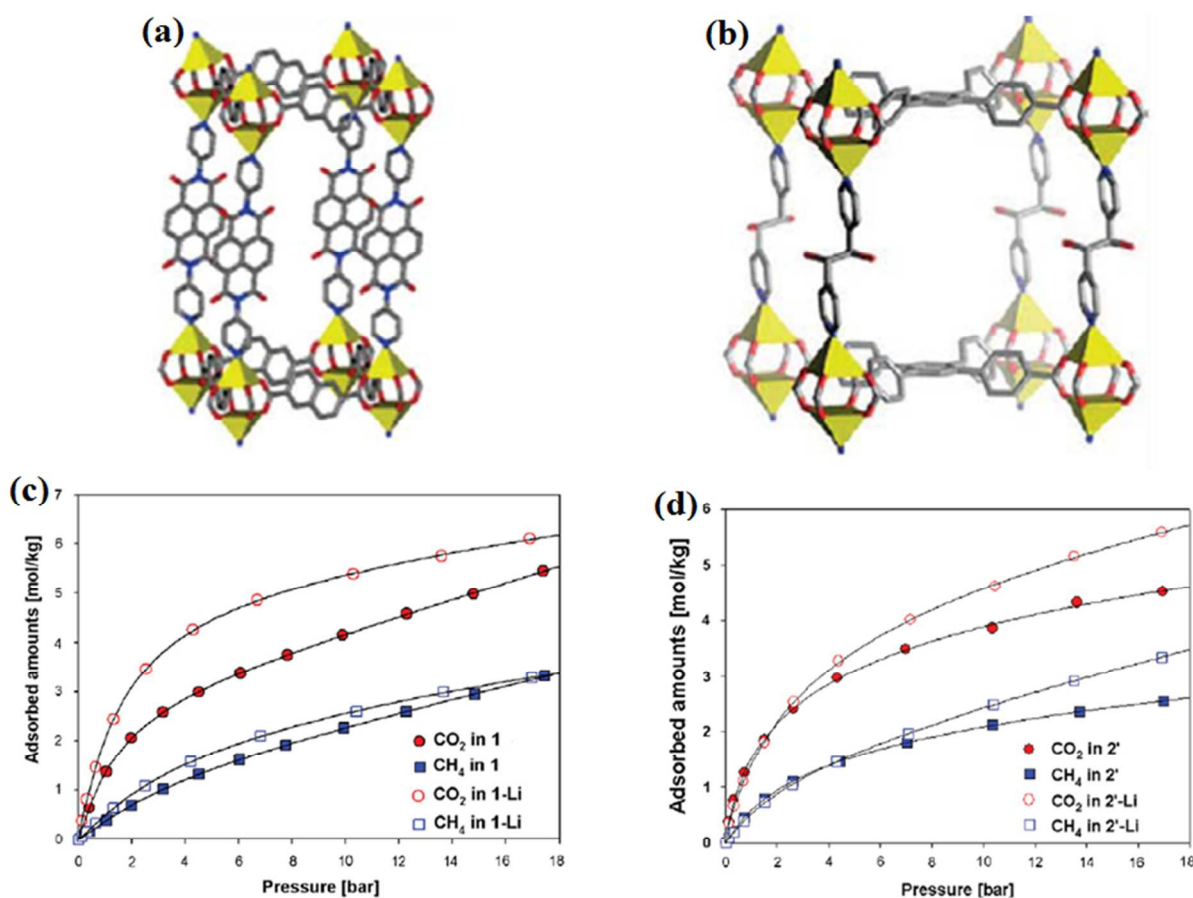


Fig. 9 (a) Crystal structure of $\{Zn_2(ndc)_2(diPyNI)\}$ omitting the interwoven second network; (b) the crystal structure of $\{Zn_2(TCPB)(DPG)\}$; (c, d) effect of chemical reduction on the CO₂ and CH₄ isotherms in $\{Zn_2(ndc)_2(diPyNI)\}$ and $\{Zn_2(TCPB)(DPG)\}$ at 298 K, respectively (solid lines are fits from the dual-site Langmuir Freundlich model). Reproduced with permission from ref. 30. Copyright[©] 2011, Elsevier.

and DPG = meso-1,2-bis(4-pyridyl)-1,2-ethanediol) was studied by Snurr *et al.* which shows structural rigidity and high thermal stability (Fig. 9a-b).³⁰ The first compound has two-fold catenated structure but second compound is a noncatenated hydroxyl-functionalized MOF. Doping of Lithium cations into the MOF $\{Zn_2(ndc)_2(diPyNI)\}$ can be made by chemical reduction of this MOF with Li metal, but in case of $\{Zn_2(TCPB)(DPG)\}$, lithium cation can be simply exchange by the proton of hydroxyl group present in DPG. In both cases Li incorporated framework showed an increased selectivity in CO_2/CH_4 sorption (Fig. 9c-d). The increases in selectivity can be explained by the favorable displacement of catenated frameworks, as well as pore-volume reduction in both the frameworks.

In a similar kind of investigation, D'Alessandro *et al.* synthesized a microporous 3D diamondoid-type four-fold interpenetrated coordination framework, $\{Zn(NDC)(DPMBI)\}$ which contains a redox-active benzenetetracarboxydiimide (pyromelliticdiimide) ligand (NDC = 2,7-naphthalene dicarboxylate and DPMBI = N,N'-di-(4-pyridylmethyl)-1,2,4,5-benzenetetracarboxydiimide) (Fig. 10a-c).³¹ Reduction with sodium naphthalenide (NaNp) of this compound produces mono radical anion of the pyromelliticdiimide ligand in the framework of $Zn(NDC)(DPMBI) \cdot Na_x$ (where x represents the molar Na^+/Zn^{2+} ratio of 0.109, 0.233, 0.367 and 0.378 from ICP-AES) which was characterized by EPR, solid state Vis-NIR spectroelectrochemistry and UV-Vis-NIR spectroscopy. With increasing stoichiometric reduction, not only the CO_2 selectivity and heat of adsorption increased but also absolute uptake of CO_2 has been significantly increased due to displacement of interpenetrated frameworks after the incorporation of Na^+ ion (Fig. 10d-e).

The discussed works clearly indicates that a simple approach of doping alkali metal in porous mixed-ligand MOFs can effectively enhance the CO_2 selectivity, and hence suggested its potential application in redox-based swing processes.

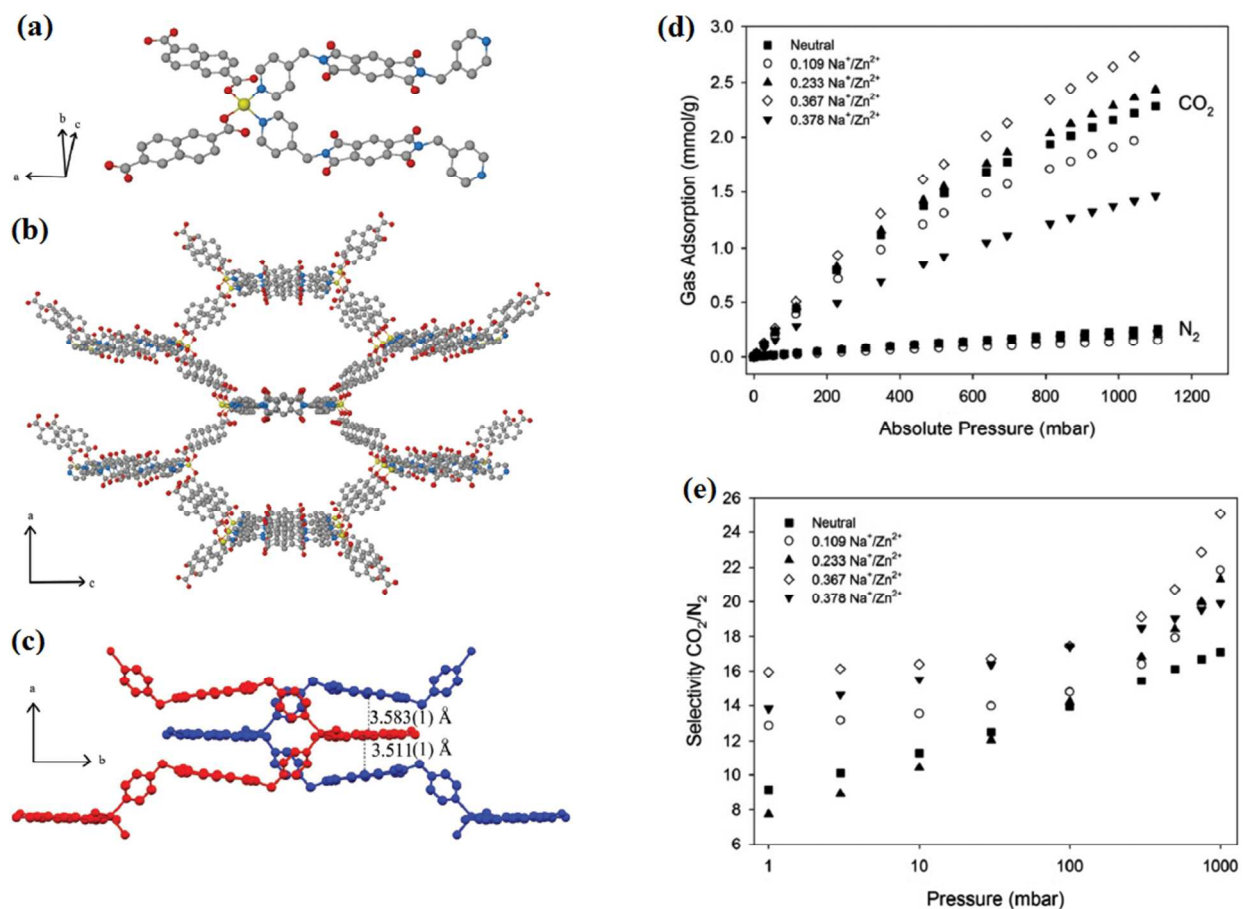


Fig. 10 (a) Ball-and-stick representations the tetrahedrally-coordinated Zn²⁺ centre of {Zn(NDC)(DPMBI)}; (b) the extended crystal structure of a single {Zn(NDC)(DPMBI)} framework viewed down the *b* axis where hydrogen atoms (DMF molecules and three of the four interpenetrated frameworks are omitted for clarity, color scheme: zinc, yellow; carbon, grey; oxygen, red; nitrogen, blue); (c) diagram of two catenated frameworks (blue and red) showing distances between the stacked DPMBI-NDC-DPMBI layers; (d) CO₂ and N₂ adsorption isotherms for {Zn(NDC)(DPMBI)} and its reduced species at 298 K; (e) IAST predicted CO₂/N₂ selectivity based on a binary 15% CO₂-85% N₂ mixture for {Zn(NDC)(DPMBI)} and its reduced species at 298 K. Reproduced from ref. 31.

4. Pore wall decoration by polar functional group

The opportunity to tailor the pore structure and functionality is perhaps the most unique advantage in the fabrication of functional MOFs. As discussed before, CO₂ show high affinity towards the polar pore surface. In fact it has been observed that by introducing polar functional groups in the linkers in the mixed ligand MOFs, CO₂ can easily be separated from gas mixture

because CO₂ has a quadrupole moment ($-1.4 \times 10^{-39} \text{ C m}^2$) while N₂, CH₄ and H₂ are entirely non-polar.³² It is needless to mention that in comparison to the aforesaid methods the tailoring of pore surface by functionalizing the ligand is pretty concentric and more success yielding methods for the selective gas adsorption. As a result, there has been several successful results of selective CO₂ have been reported in the literature.³³ In case of mixed ligand MOFs, chemical environment of the pore surface can far better be tuned by introducing different polar functional groups in two linkers. Hence we will discuss this method in four different sections depending on the nature of the polar functional groups.

(i) Pore wall decorated by fluorine

Fluorine being the most electronegative element in the periodic table could be very much useful to create a polar environment within the pore of the MOF. Thus researchers of this area have explored the prospect of synthesizing fluorinated metal organic frameworks (F-MOFs), using fluorinated polycarboxylate ligands with porous surfaces, and bare fluorine atoms for CO₂ separation. There are some reports on the possibility of synthesizing fluorinated mixed ligand metal organic frameworks using fluorinated polycarboxylate ligands along with N,N'-donor ligand.

Bharadwaj *et al.* synthesized a porous three-dimensional (3D) metal–organic framework of Zn(II), $\{[\text{Zn}_4\text{O}(\text{bfbpdc})_3(\text{bpy})_{0.5}(\text{H}_2\text{O})] \cdot (3\text{DMF})(\text{H}_2\text{O})\}_n$, from fluorinated linear rigid ligand, 2,2'-bistrifluoromethyl-biphenyl-4,4'-dicarboxylate (bfbpdc) and colinker 4,4'-bipyridine (bpy) using solvothermal technique (Fig. 11a-b).³⁴ The crystal structure of MOF revealed that it contains two rectangular channels along (001) and (110) direction with dimensions $10.76 \times 8.94 \text{ \AA}^2$ and $7.91 \times 4.54 \text{ \AA}^2$, respectively (Fig. 11b). The channels decorated with pendant trifluoromethyl groups of bfbpdc²⁻ linker, resulting highly polar pore surfaces and a surface area of $1450 \text{ m}^2 \text{ g}^{-1}$. The $-\text{CF}_3$ group on the pore surface induces a polarized environment and strong acid–base interaction with acidic guests like CO₂. The CO₂ uptake of this compound is $315 \text{ cm}^3 \text{ g}^{-1}$ at 195 K and 1 bar. The CO₂ uptakes at different temperature are $20 \text{ cm}^3 \text{ g}^{-1}$, $14.9 \text{ cm}^3 \text{ g}^{-1}$, and $11 \text{ cm}^3 \text{ g}^{-1}$, at 262 K, 273 K and 283 K respectively and the isosteric heat of CO₂ adsorption is 21.8 kJ mol^{-1} (Fig. 11c-d).

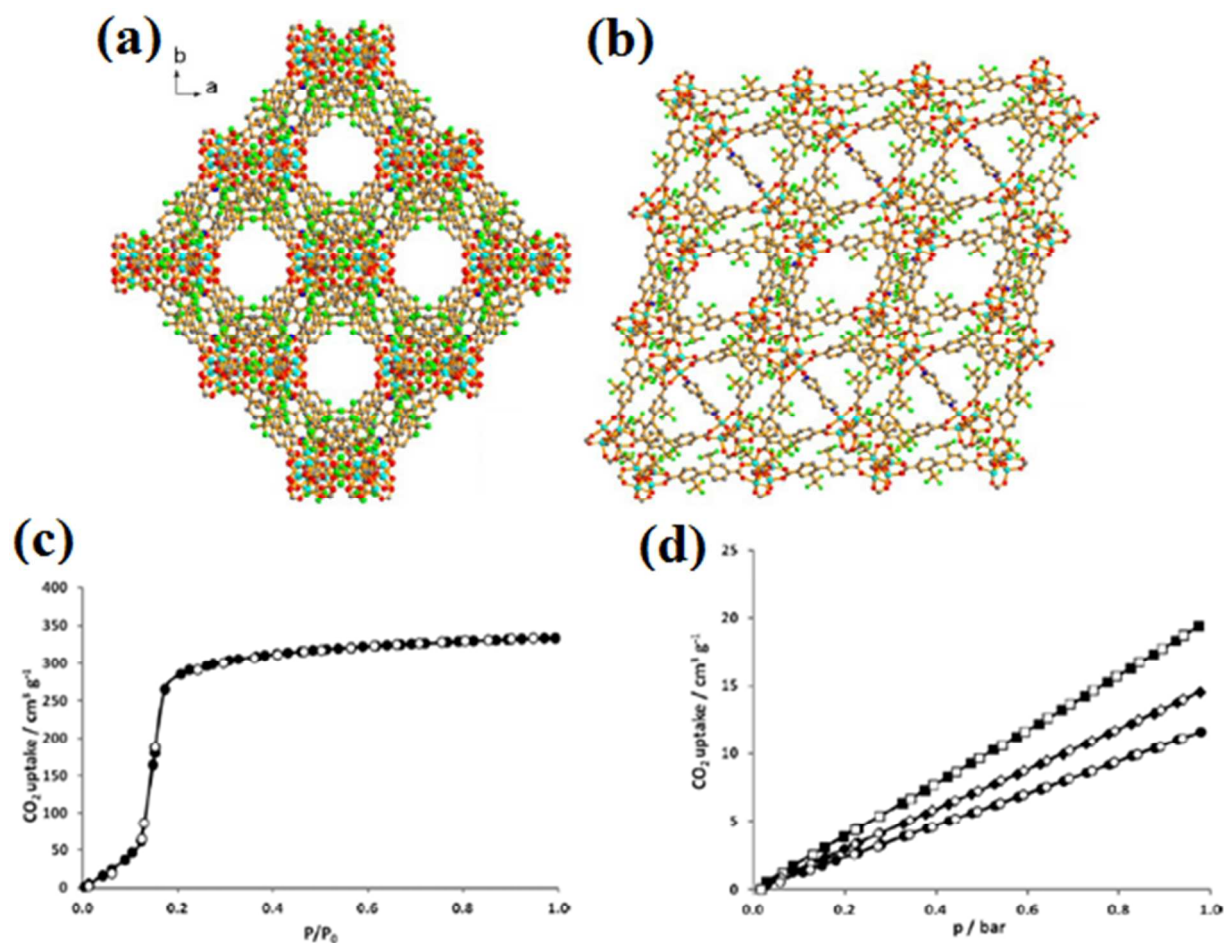


Fig. 11 (a) View of the 3D framework of $\{[\text{Zn}_4\text{O}(\text{bfbpdc})_3(\text{bpy})_{0.5}(\text{H}_2\text{O})] \cdot (3\text{DMF})(\text{H}_2\text{O})\}_n$, along the *c* axis showing rectangular shaped channels decorated with pendent trifluoromethyl groups; (b) rectangular channels along the (110) direction decorated with pendent trifluoromethyl groups (hydrogen atoms are omitted for clarity); (c) carbon dioxide physisorption isotherms of activated $\{[\text{Zn}_4\text{O}(\text{bfbpdc})_3(\text{bpy})_{0.5}(\text{H}_2\text{O})] \cdot (3\text{DMF})(\text{H}_2\text{O})\}_n$ at 196 K (adsorption/desorption ●/○); (d) carbon dioxide physisorption isotherms of activated $\{[\text{Zn}_4\text{O}(\text{bfbpdc})_3(\text{bpy})_{0.5}(\text{H}_2\text{O})] \cdot (3\text{DMF})(\text{H}_2\text{O})\}_n$ up to 1 bar at 283 K (circles), 273 K (diamonds), and 262 K (squares). Reproduced with permission from ref. 34. Copyright© 2013, American Chemical Society.

A series of isostructural porous MOFs were reported by Bu and co-workers, which are prepared by the reaction of Ni(II) with 2,4,6-tri(4-pyridinyl)-1,3,5-triazine (tpt) and different functionalized (-H, -NH₂, -NO₂, and -F) *o*-phthalic acid (OPA) as co-ligand (Fig. 12a).³⁵ Crystallographic analysis reveals that all structures reveal a three dimensional (3D) porous

framework with chiral channels decorated with functional group. MOFs with fluorine atoms in different number and position (TKL-104–TKL-107) show high stability and have nice selectivity for CO₂ capture over N₂ and CH₄. The amounts of uptake of CO₂ of the fluorinated MOFs (at 273 K and 1.2 bar) are 33 cm³ g⁻¹ for TKL-104, 105 cm³ g⁻¹ for TKL-105, 126 cm³ g⁻¹ for TKL-106, and 150 cm³ g⁻¹ for TKL-107.

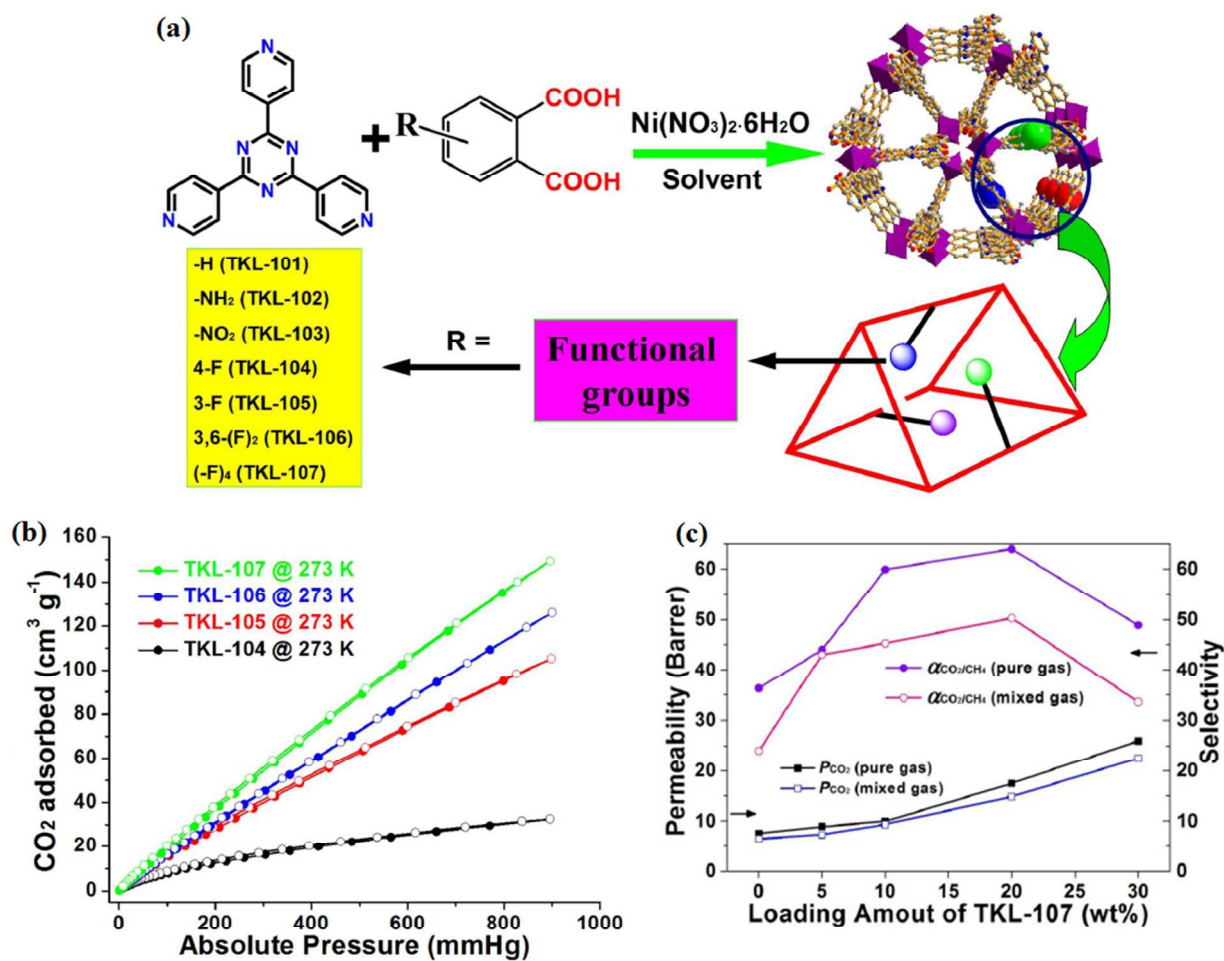


Fig. 12 (a) Schematic presentation of general route for the synthesis of TKL MOFs; (b) CO₂ adsorption isotherms at 273 K; (c) CO₂/CH₄ selectivity and permeability trend of the TKL-107 MMMs towards pure gas and mixed gas. Reprinted by permission from Macmillan Publishers Ltd: Scientific Reports, ref. 35. Copyright[©] 2013.

The high CO₂ uptake and selectivity over N₂ and CH₄ make these fluorine functionalized MOFs good candidates for the sequestration of CO₂. Moreover, for the better exploration of potential applications of MOFs towards CO₂ separation from gas mixture, TKL-107-doped mixed matrix

membranes (MMMs) were prepared and the CO₂/CH₄ permeation experiments show 64.6 and 50.3 for the selectivity on 20% loading (Fig. 12b-c).

(ii) Pore wall decorated by amino group

Amine is the oldest tools among the available chemical process which people have been extensively used to trap CO₂ in terms of amine scrubbing.^{3a} Grafting of amines or nitrogen hetero cycle onto the pore surfaces of mixed MOFs is an attempt to improvise such technique within the MOF and can certainly improve both the adsorption capacity and the selectivity of CO₂ due to the Lewis base-acid interaction between the NH₂ and CO₂, which has also been supported by some theoretical results too.^{33c}

Shimizu *et al.* reported a zinc aminotriazolato oxalate MOF {Zn₂(atz)₂(ox)} (atz = 3-amino-1,2,4-triazole and ox = oxalate) with amine-lined pores, exhibiting very high CO₂ uptake and adsorption enthalpy.^{36a} The aminotriazolato ligands bind to zinc centers in a tridentate fashion forming Zn-aminotriazolato layers whereas the amino groups remain uncoordinated. These layers are pillared by oxalate forming a three-dimensional framework with amino group decorated within the 2D channels (Fig. 13a-b). The adsorption experiments carried out at 273K and 293 K revealed that the framework shows high selectivity for CO₂ whose uptake capacities are ~97.5 cm³/g and 84.8 cm³/g; whereas there is almost no uptake for N₂, H₂ and Ar (Fig. 13c). They also observed crystallographically, the direct binding of CO₂ with Zn₂(Atz)₂(ox) framework at low pressure of CO₂ (Fig. 13d-f).^{36b} The crystal structural refinement indicates two independent CO₂ binding sites were located within each pore of the MOF: one is near the free amine group, and other is closer to the oxalates. The CO₂ could interact with an amine either way *via* N-H...O hydrogen bonding or *via* an interaction between the lone pair of N and the C atom of CO₂ making the CO₂ amine interaction highly probable. Using these experimental result and molecular simulation studies they suggested that the actual reason is appropriate pore size, strong interaction between CO₂ and functional groups on the pore surface, and cooperative binding of CO₂ molecules for huge uptake of CO₂ at low pressure in Zn₂(Atz)₂(ox).

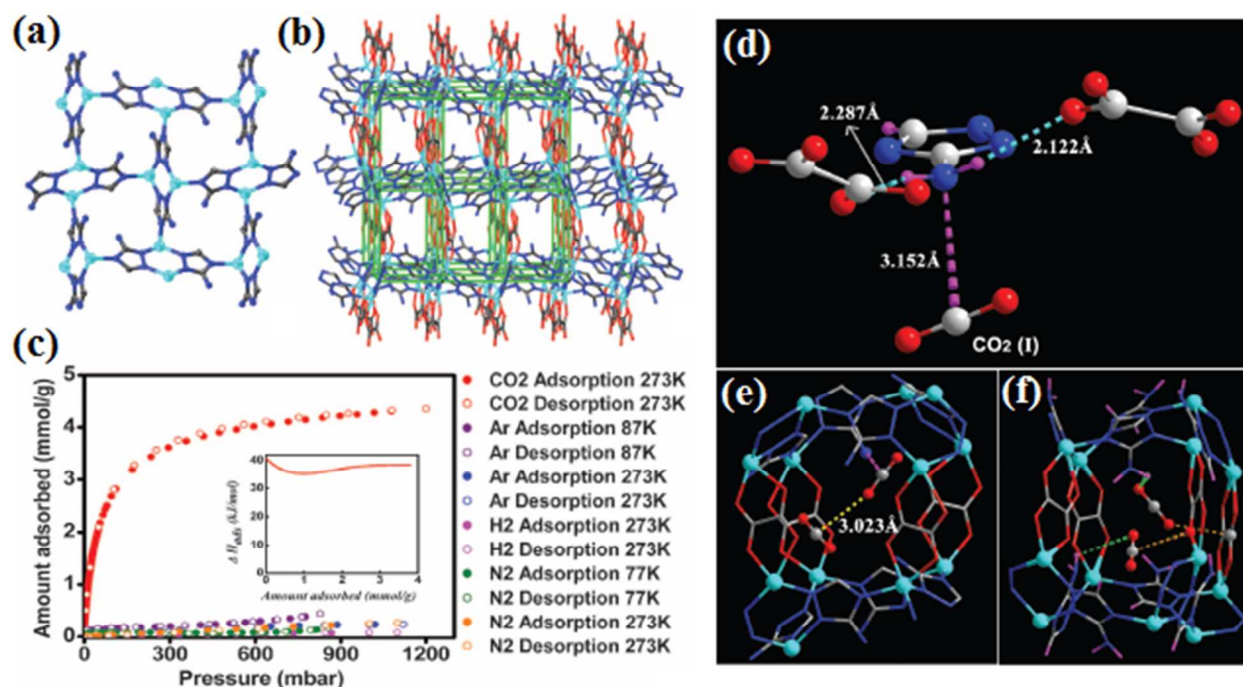


Fig. 13 (a) Structure of the Zn-Atz layer in $\text{Zn}_2(\text{Atz})_2(\text{ox})$ (Zn, cyan; C, black; N, blue; H, not shown); (b) three-dimensional structure of $\text{Zn}_2(\text{Atz})_2(\text{ox})$, wherein the Zn-Atz layers are pillared by oxalate moieties (O, red) to form a six-connected cubic network shown as green struts; (c) adsorption isotherms for different gases carried out using $\text{Zn}_2(\text{Atz})_2(\text{ox})$, inset shows heat-of-adsorption data calculated with the CO_2 isotherms measured at 273 K; (d, e, f) the CO_2 binding (directly determined by X-ray structure refinement at 173 K) within the pores of $\text{Zn}_2(\text{Atz})_2(\text{ox})$. From ref. 36b. Reprinted with permission from AAAS.

An anionic porous framework, $[(\text{CH}_3)_2\text{NH}_2][\text{Zn}_3(\text{DATRZ})(\text{BDC})_3] \cdot x\text{DMF}$ (DATRZ = 3,5-diamino-1,2,4-triazole, BDC = 1,4-benzenedicarboxylate, DMF = N,N-dimethylformamide) with amine-decorated polyhedral cages has reported by Feng *et al* (Fig. 14a-d).³⁷ The crystal structure of this anionic framework showed that the four carboxylate groups of BDC ligands coordinated to two Zn(II) centers, forming a $[\text{Zn}_2(\text{CO}_2)_4]$ paddle-wheel secondary building unit (SBU), whereas, one DATRZ ligand joins two metal centers together with two carboxylate groups of BDC, generating a novel $[\text{Zn}_2(\text{CO}_2)_2(\text{DATRZ})]$ triazole-carboxylate SBU. The octahedral and trigonal bipyramidal SBUs join each other to form a (5,6)-connected three-dimensional framework (Fig. 14a-d). The amine groups are just situated in the windows of each polyhedral cage. The CO_2 uptakes of this compound are 22.8 and 15.9 wt. % respectively at 273 K and 298 K under 1 atm, respectively with isosteric heat of adsorption value of ~ 28.2 kJ/mol.

This compound also exhibits pretty high CO₂/N₂ and CO₂/CH₄ selectivity (31:1 for CO₂ : N₂, and 5:1 for CO₂ : CH₄ at 0 °C, 1 atm) (Fig. 14e).

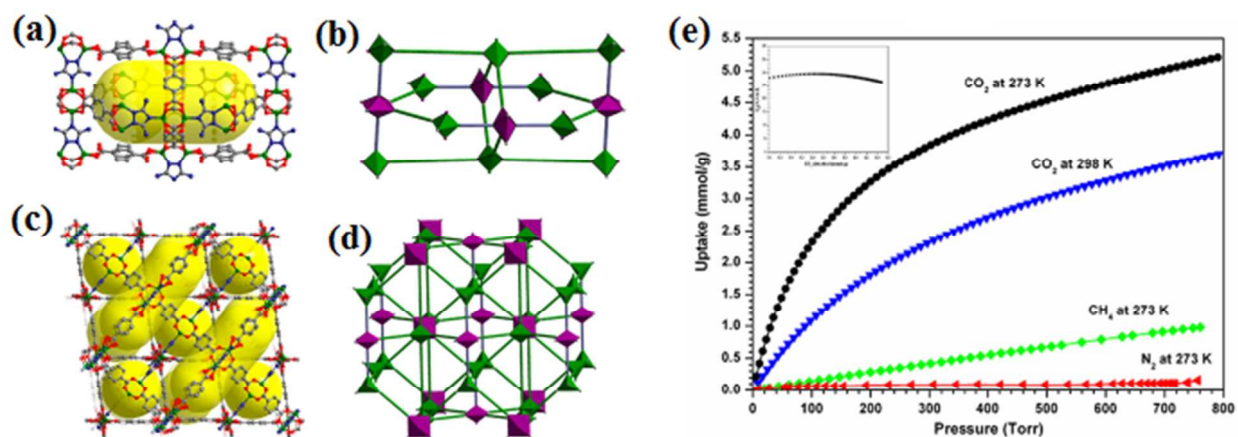


Fig. 14 (a) Nanoscopic cage in [(CH₃)₂NH₂][Zn₃(DATRZ)(BDC)₃] \cdot xDMF; (b) polyhedral representation of the nanoscopic cage; (c) 3D framework of [(CH₃)₂NH₂][Zn₃(DATRZ)(BDC)₃] \cdot xDMF; (d) polyhedral representation of the 3D framework; (e) CO₂, CH₄, and N₂ isotherms at 273 or 298 K, inset shows the enthalpy of adsorption (Q_{st}) as a function of CO₂ uptake. Reproduced with permission from ref. 37. Copyright[©] 2012, American Chemical Society.

Recently, Maji *et al.* synthesized two isomeric supramolecular mixed ligand MOFs of Cd(II), {[Cd(NH₂-bdc)(bphz)_{0.5}] \cdot DMF \cdot H₂O}_n (NH₂-bdc = 2-aminobenzenedicarboxylic acid, bphz = 1,2-bis(4-pyridylmethylene)hydrazine) (Fig. 15a-b).³⁸ Structural isomerism is based on two different secondary building units (SBUs); the first isomer having the paddle-wheel-type Cd₂(COO)₄ SBU, which is flexible in nature; while the other isomer has μ -oxo-bridged Cd₂(μ -OCO)₂ rigid SBU. In both cases paddle-wheel and oxo-bridged SBUs are connected by the NH₂-bdc linker and form 2D square grids that are pillared by the bphz linker forming a 3D α -polonium-type pillared-layer porous framework. Both frameworks are two-fold interpenetrated containing rectangular channels and the pore surface is decorated with pendant -NH₂ and =N-N= functional groups (Fig. 15a-b). At 195 K, both frameworks selectively adsorb CO₂ over other gases (N₂, O₂, H₂, and Ar) due to the strong interaction of CO₂ with the -NH₂ and =N-N= functionalized pore surface and these are also corroborated by the DFT calculations (Fig. 15c-d).

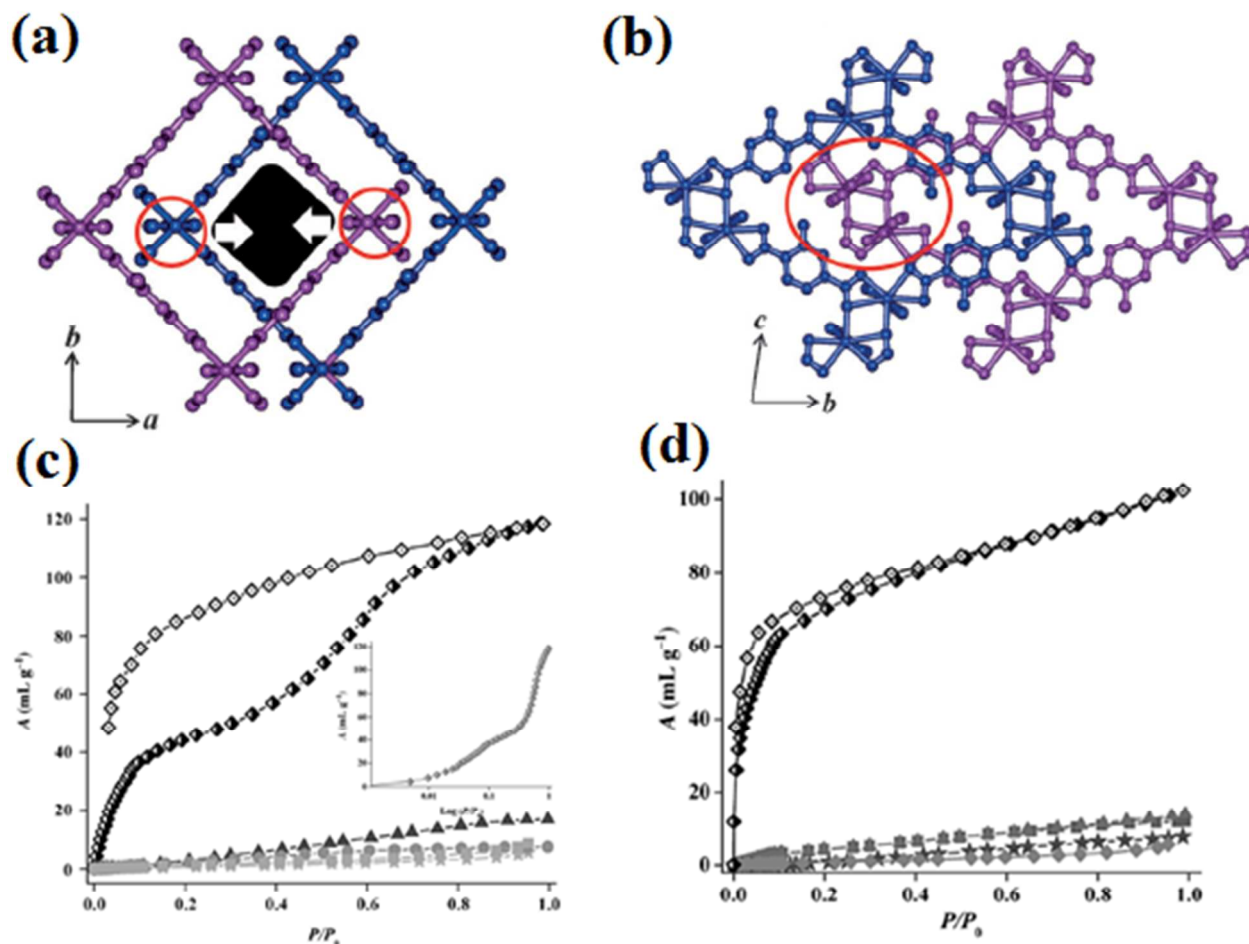


Fig. 15 (a, b) View of interpenetrated net of supramolecular isomers $\{[\text{Cd}(\text{NH}_2\text{-bdc})(\text{bphz})_{0.5}]\cdot\text{DMF}\cdot\text{H}_2\text{O}\}_n$ having paddle wheel and oxo-bridged SBU along the *c* axis and *a* axis, respectively; (c, d) adsorption isotherms supramolecular isomers $\{[\text{Cd}(\text{NH}_2\text{-bdc})(\text{bphz})_{0.5}]\cdot\text{DMF}\cdot\text{H}_2\text{O}\}_n$ containing paddle wheel and oxo-bridged SBU at 195 K: CO₂ adsorption (half-filled diamonds), CO₂ desorption (open diamonds), N₂ (stars), H₂ (circles), Ar (triangles), O₂ (squares); inset: CO₂ adsorption profile at 195 K (log scale). Reproduced with permission from ref. 38. Copyright© 2014, WILEY-VCH Verlag GmbH & Co. KGaA, Weinheim.

The influence of amino group on enhancement of the adsorption and selectivity of CO₂ in mixed metal–organic frameworks has also shown very recently by Koner *et al.* They prepared two isorecticular Cd(II) based MOFs of benzene dicarboxylic acid (bdc) and amino functionalized benzene dicarboxylic acid (2-NH₂bdc), $\{[\text{Cd}(\text{bdc})(4\text{-bpmh})]\}_n\cdot 2n(\text{H}_2\text{O})$ and $\{[\text{Cd}(2\text{-NH}_2\text{bdc})(4\text{-bpmh})]\}_n\cdot 2n(\text{H}_2\text{O})$ with a linear N,N'-donor ligand (4-bpmh) [2-NH₂bdc = 2-amino benzene

dicarboxylic acid and 4-bpmh = N,N-bis-pyridin-4-ylmethylene-hydrazine] (Fig. 16a).^{19g} Both the compounds have similar two-fold interpenetrated 3D structure. In both cases, two-dimensional square grids of metal-carboxylate are pillared by 4-bpmh linkers along *b* axis forming 3D framework and each 3D framework is interpenetrated with another, resulting in two-fold interpenetrated architecture.

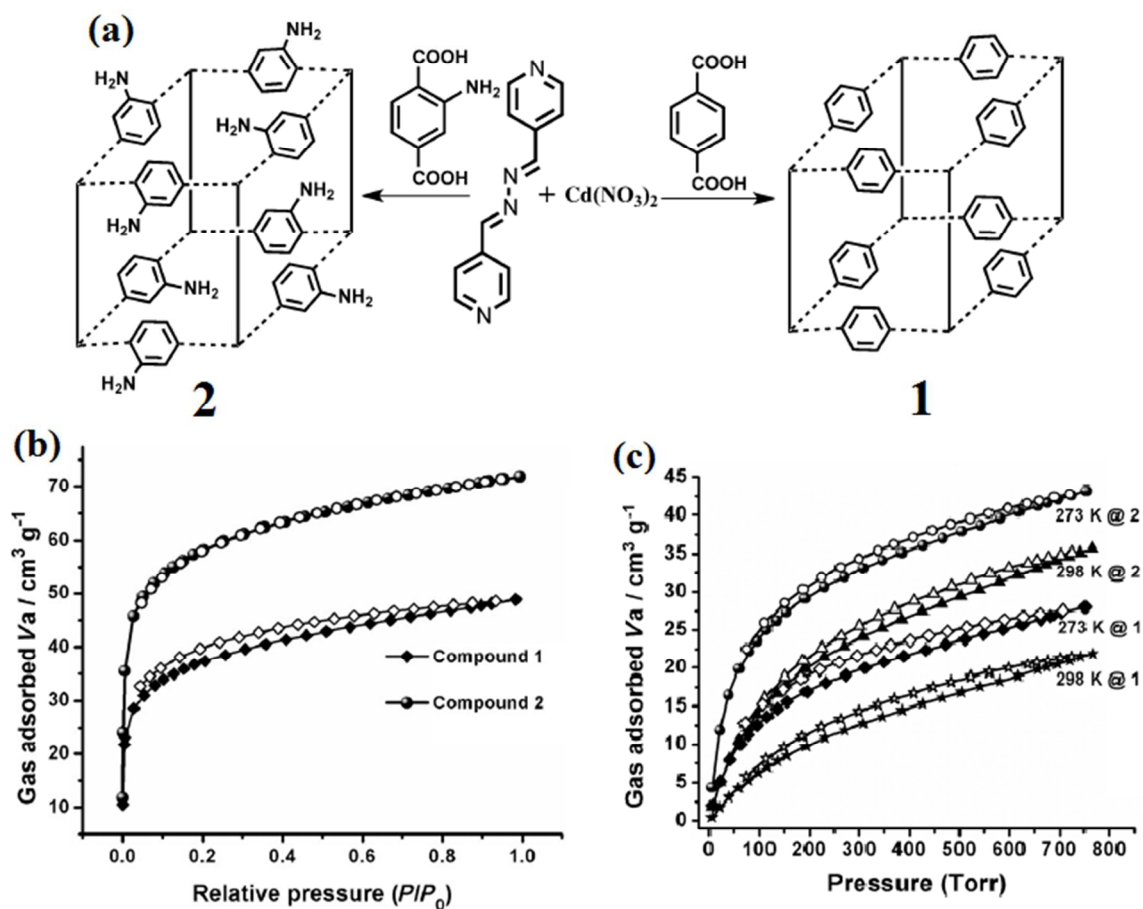


Fig. 16 (a) Schematic view of the comparative synthesis of $\{[\text{Cd}(\text{bdc})(4\text{-bpmh})]\}_n \cdot 2n(\text{H}_2\text{O})$ and $\{[\text{Cd}(2\text{-NH}_2\text{bdc})(4\text{-bpmh})]\}_n \cdot 2n(\text{H}_2\text{O})$; (b) sorption isotherms of CO₂ for compounds $\{[\text{Cd}(\text{bdc})(4\text{-bpmh})]\}_n \cdot 2n(\text{H}_2\text{O})$ (diamonds) and $\{[\text{Cd}(2\text{-NH}_2\text{bdc})(4\text{-bpmh})]\}_n \cdot 2n(\text{H}_2\text{O})$ (circles) measured at 195 K; (c) sorption isotherms of CO₂ for compounds $\{[\text{Cd}(\text{bdc})(4\text{-bpmh})]\}_n \cdot 2n(\text{H}_2\text{O})$ (diamonds and star) and $\{[\text{Cd}(2\text{-NH}_2\text{bdc})(4\text{-bpmh})]\}_n \cdot 2n(\text{H}_2\text{O})$ (circles and triangles) measured at 273 and 298 K, respectively (filled and open circles represent adsorption and desorption respectively). Reproduced with permission from ref. 19g. Copyright© 2015, WILEY-VCH Verlag GmbH & Co. KGaA, Weinheim.

The non-functionalized framework shows CO₂ uptake of 48.9 cm³ g⁻¹, whereas amine-functionalized framework exhibits 71.6 cm³ g⁻¹ CO₂ uptakes at 195 K and 1 bar pressure. It is interesting to note that the CO₂ uptake of amine-functionalized framework is approximately twice than that of the non-functionalized one. At 298 K also the same CO₂ adsorption trend is followed, showing approximately 4.3 wt % and 7.0 wt % of CO₂, for the non-functionalized and amine-functionalized variant respectively, signifying the importance of presence of amino functional groups in the linkers for the improvement of the CO₂ uptake capacity of the MOF (Fig. 16b-c).

(iii) Pore wall decorated by amide group

Like the amine functionality, the amide group can also be interacted with the CO₂ molecules by NC=O...CO₂ and NH...OCO interactions, and may be useful for the construction of MOF with selective CO₂ adsorption properties. Due to the high affinity of the amide based linkers towards metal ion, it is bit difficult to construct a mixed ligand MOF with amide functionalized linkers. As a result, the numbers of mixed ligand MOF with amide functionalized pore wall are very limited.

Lu *et al* reported a two-fold interpenetrated mixed MOF of Zn(II), {[Zn₄(1,4-bdc)₄(bpda)₄·5DMF·3H₂O]}_n by using 1,4-benzene dicarboxylate (1,4-bdc) and N,N'-bis(pyridine-4-yl)-1,4-benzenedicarboxamide (bpda) (Fig. 17a-b).³⁹ The solid-state structure of the MOF indicates the presence of 2D layers formed by the linking of Zn₂(COO)₄ through 1,4-bdc and amide pillars (bpda) connect the grids to form 3D two-fold interpenetrated frameworks. The framework has two different channels decorated by amide functional groups with effective dimensions of 2 × 3 Å² and 3 × 9 Å² (Fig. 17a-b). The pore surface seems to be highly polar due to the presence of amide group in the channels and that is reflected in the adsorption studies. The Langmuir surface area of the framework is ~468 m²/g calculated from CO₂ adsorption. The amide-functionalized MOF preferentially adsorbs CO₂ over nitrogen at low pressures with a heat of adsorption value 30.2 kJ mol⁻¹ (Fig. 17c-d). It is interesting to note that the amount of captured CO₂ at 1 bar pressure is almost equivalent to the number of bare amide groups of the framework and also supported by theoretical calculation.

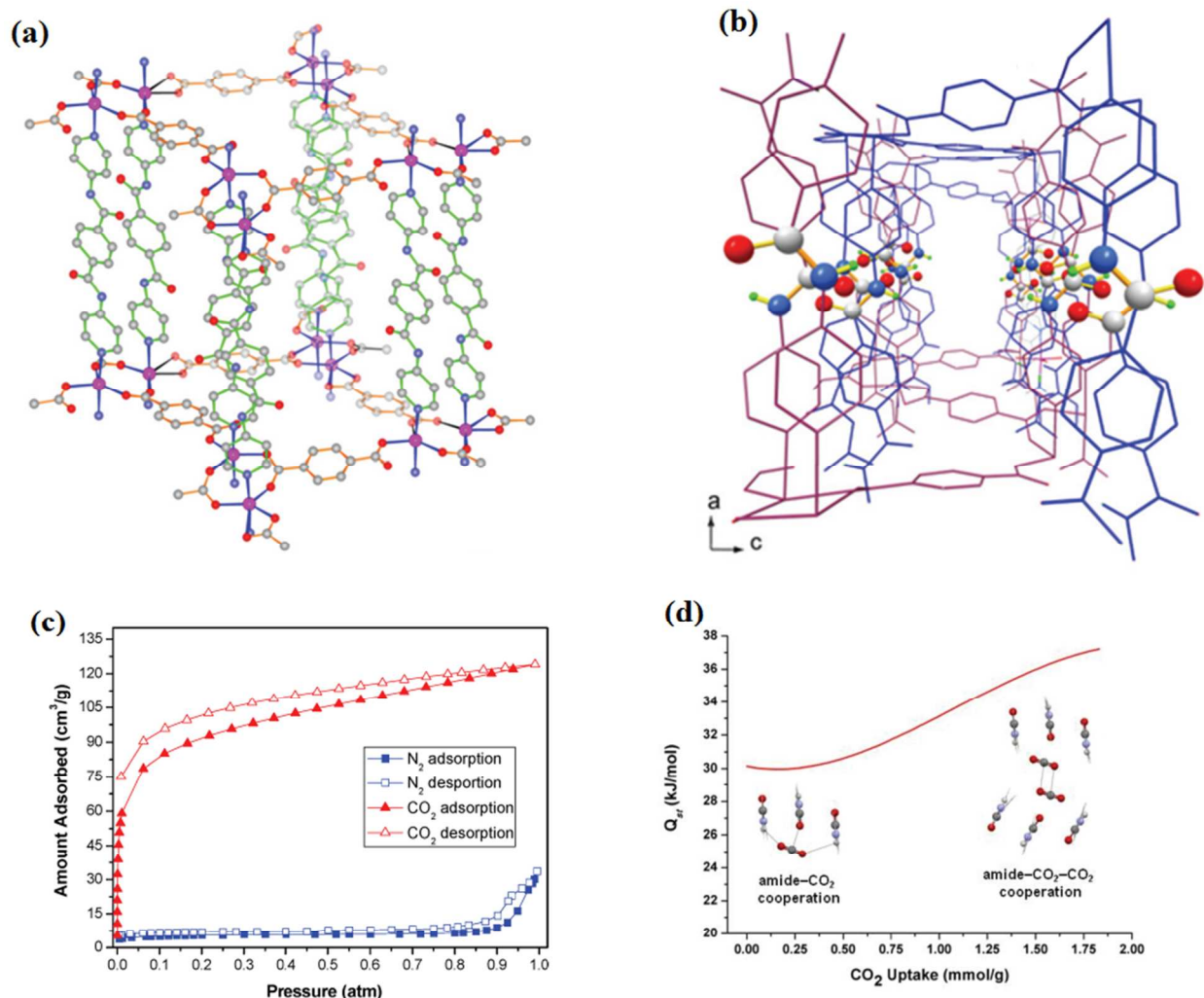


Fig. 17 (a) Side view of an α -polonium-type cage of $\{[Zn_4(1,4-bdc)_4(bpda)_4] \cdot 5DMF \cdot 3H_2O\}_n$; (b) spotlight of the larger channel opening showing a nearly unique arrangement of the unsheltered amide groups in $\{[Zn_4(1,4-bdc)_4(bpda)_4] \cdot 5DMF \cdot 3H_2O\}_n$; (c) adsorption isotherms of N₂ and CO₂ measured of $\{[Zn_4(1,4-bdc)_4(bpda)_4] \cdot 5DMF \cdot 3H_2O\}_n$ at 77 and 195 K, respectively; (d) isosteric heat (Q_{st}) of CO₂ adsorption of $\{[Zn_4(1,4-bdc)_4(bpda)_4] \cdot 5DMF \cdot 3H_2O\}_n$. Reproduced with permission from ref. 39. Copyright © 2013, American Chemical Society.

Wang *et al.* prepared an acylamide-functionalized 3D microporous metal-organic framework of Zn(II); $[Zn_2(bcta)(dipy)(\mu_2-OH)] \cdot 2DMF \cdot H_2O$, by using 4,4',4''-[1,3,5-benzenetriyltris(carbonylimino)]trisbenzoate acid (H₃bcta) and the long rigid 1,2-di(4-pyridyl)ethylene (dipy) as a pillared linker (Fig. 18a-b).⁴⁰ The 3-D framework is built here by the pillaring of 2D Zn-bcta honeycomb layer with the dipy ligand and shows an unprecedented 2D \rightarrow 3D polycatenation. The 2D \rightarrow 3D polycatenated framework contains open channels having

bare amide group with dimensions of approximately $4.4 \times 4.1 \text{ \AA}^2$ (Fig. 18a-b). The desolvated framework of the compound selectively adsorbs CO_2 at room temperature over N_2 with high heat of adsorption (30.2 kJ mol^{-1}) (Fig. 18c-d). The high selectivity of CO_2 is due to the high dipole–quadrupole interactions between the $-\text{CONH}-$ groups of the framework and CO_2 , as mentioned earlier.

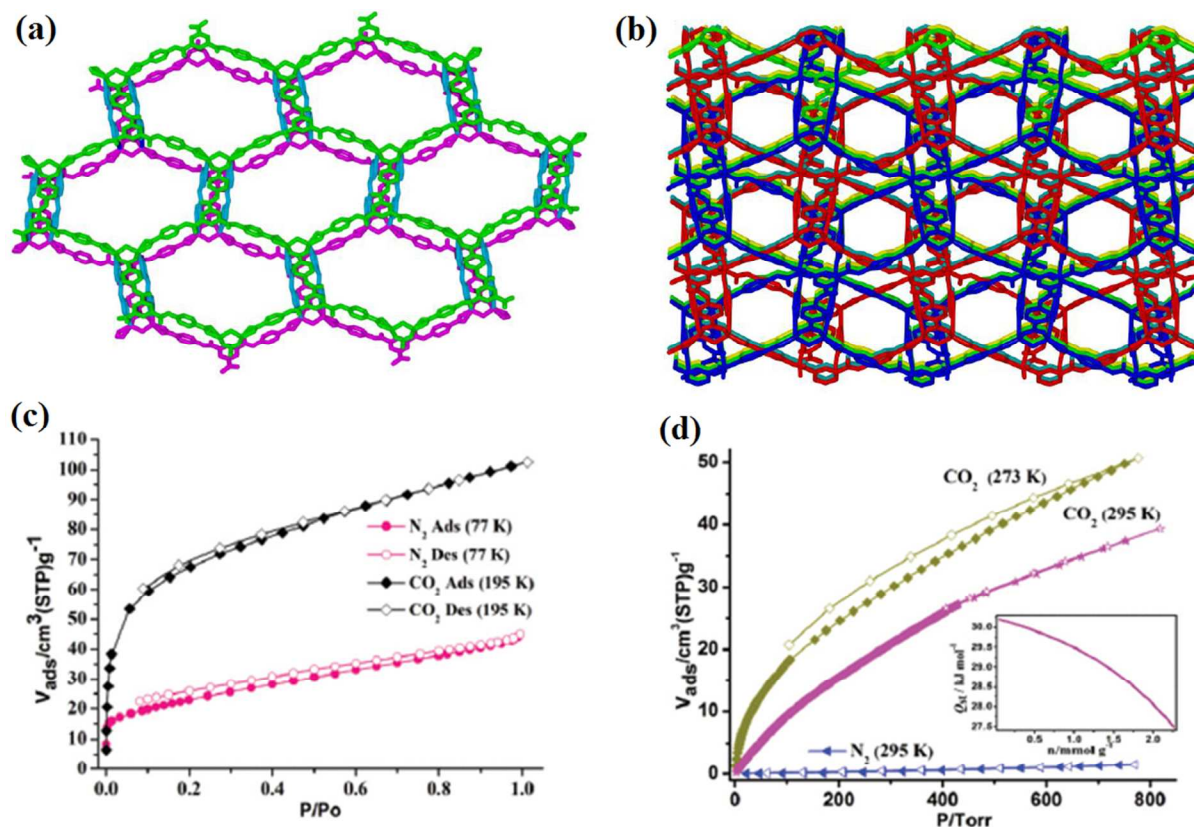


Fig. 18 (a) View of simplified net of the the two layers are connected by dipy to generate a bilayer; (b) View of the 2D \rightarrow 3D polycatenation array: each color presents one bilayer net; (c) N_2 (77 K) and CO_2 (195 K) sorption isotherms; (d) N_2 (295 K), CO_2 (273 and 295 K) sorption isotherms. The inset shows the CO_2 adsorption heat. Reproduced from ref. 40.

Another interesting example of enhanced CO_2 uptake and CO_2/CH_4 selectivity by amide functionalization in mixed ligand MOFs was given by Bu *et al.* They prepared two mixed ligand MOFs; $\{[\text{Zn}_4(\text{bpta})_2(4\text{-pna})_2(\text{H}_2\text{O})_2] \cdot 4\text{DMF} \cdot 3\text{H}_2\text{O}\}_n$ and $\{[\text{Zn}_2(\text{bpta})(\text{bpy}\text{-ea})(\text{H}_2\text{O})] \cdot 2\text{DMF} \cdot \text{H}_2\text{O}\}_n$ by using two different pillar ligands N-(4-pyridyl)isonicotinamide (4-pna) and 1,2-bis(4-pyridyl)ethane (bpy-ea) with 2,2',6,6'-tetracarboxylic acid (H_4bpta) acid (Fig. 19a-b).^{19h} The structure of both compounds are almost same and in both the cases Zn-bpta layers are pillared by

4-pna and bpy-ea ligands forming 3D pillared frameworks containing channels filled with H₂O and DMF molecules (Fig. 19a-b). CO₂ adsorption studies at 900 mmHg pressure reveals that the amide functionalized MOF, {[Zn₄(bpta)₂(4-pna)₂(H₂O)₂].4DMF.3H₂O}_n adsorbs (60.31 and 41.95 cm⁻³ g⁻¹ at 273 K and 298 K respectively) much high amount of CO₂ than the non functionalized {[Zn₂(bpta)(bpy-ea)-(H₂O)].2DMF.H₂O}_n (20.51 and 14.89 cm⁻³ g⁻¹ at 273 K and 298 K respectively) (Fig. 19c). The heat of adsorption value (Q_{st}) for CO₂ of amide functionalized MOF is 34.82 kJ mol⁻¹ at zero loading, while the Q_{st} value of non-functionalized one is 27.69 kJ mol⁻¹ (Fig. 19d). The amide functionalized MOF also shows high CO₂/CH₄ selectivity than non functionalized variant.

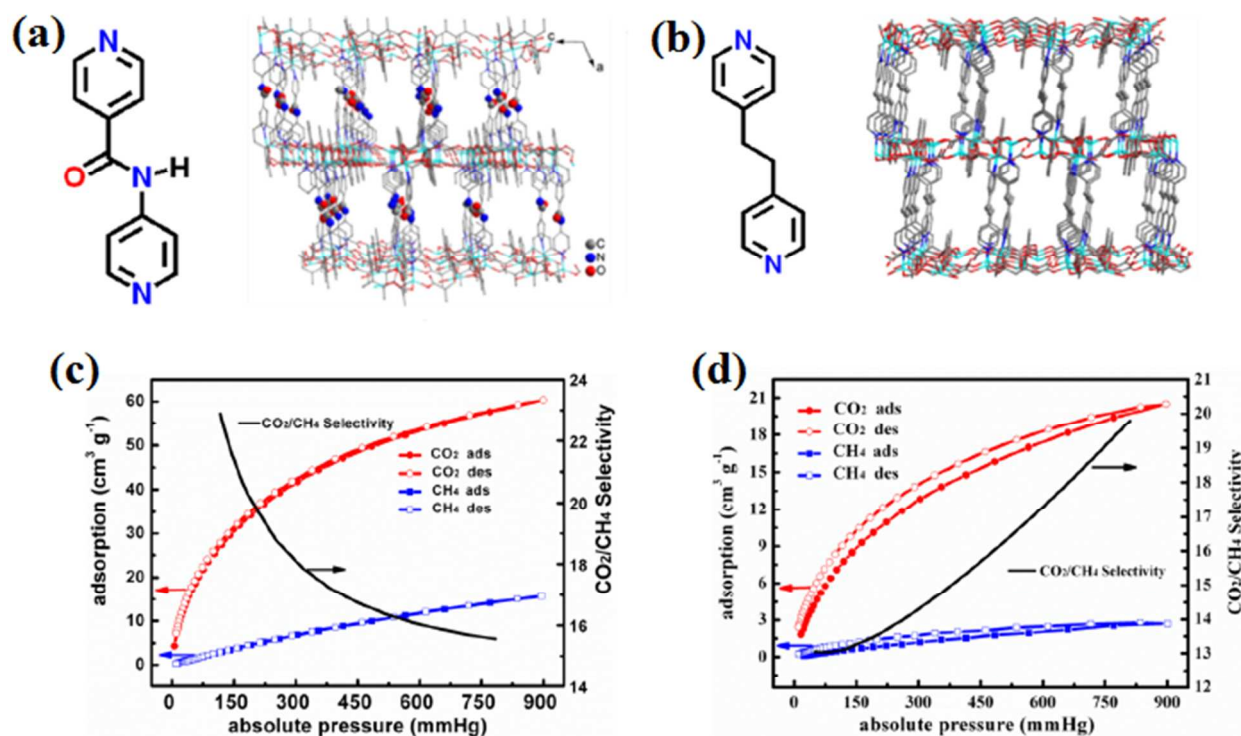


Fig. 19 (a) Views in parallel with the channels along the *b* direction of {[Zn₄(bpta)₂(4-pna)₂(H₂O)₂].4DMF.3H₂O}_n; (b) views in parallel with the channels along the *b* direction of {[Zn₂(bpta)(bpy-ea)-(H₂O)].2DMF.H₂O}_n; (c, d) CO₂ and CH₄ adsorption and the selectivity for CO₂ from an equimolar mixture of CO₂ and CH₄ for complexes {[Zn₄(bpta)₂(4-pna)₂(H₂O)₂].4DMF.3H₂O}_n and {[Zn₂(bpta)(bpy-ea)-(H₂O)].2DMF.H₂O}_n at 273 K, respectively. Reproduced with permission from ref. 19h. Copyright © 2014, American Chemical Society.

The comparatively high Q_{st} value of amide functionalized MOF can be ascribed to the interaction between CO_2 molecules and the polar acylamide groups, which could facilitate the capture and selectivity of CO_2 .

(iv) Pore wall decorated by azo/azine functional group

It is evident from the above discussion that the inclusion of amine and amide into the porous framework is bit tricky and thus an alternate approach of incorporating azo/azine functional group in the pore wall become very popular nowadays for creating polar pore for the selective adsorption of CO_2 . It is needless to mention the synthetic ease and stability of such azo/azine based linkers make them useful for the fabrication of mixed ligand framework particularly when they used in combination with the robust dicarboxylate.

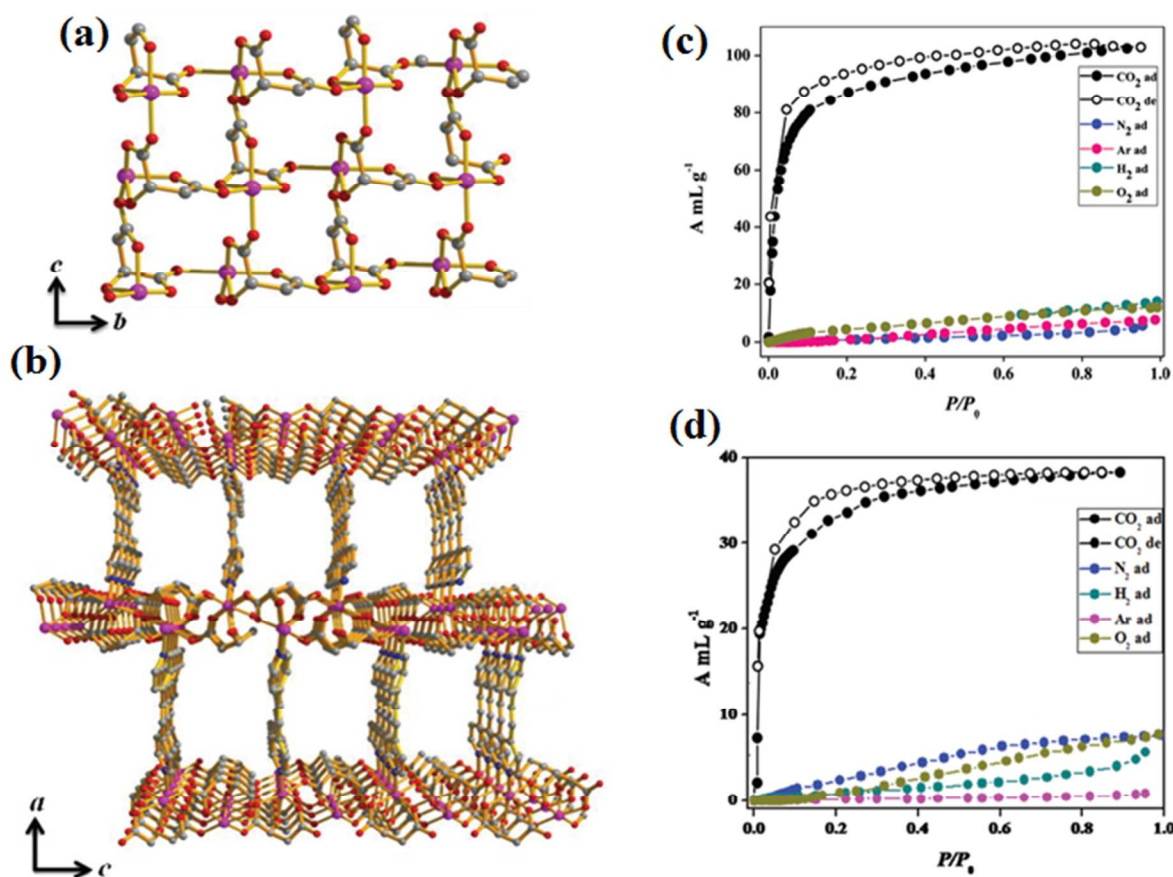


Fig. 20 (a) View of the 2D sheet of $[M-L-malate]_n$ in the crystallographic bc plane; (b) view of the 3D pillared-layer framework of $\{[M(L-mal)(azpy)_{0.5}] \cdot 2H_2O\}_n$ ($M = Co/Ni$) showing 1D rectangular channels along the b axis; (c) adsorption studies of different gases for compound $\{[Co(L-mal)(azpy)_{0.5}]\}_n$; (d) adsorption studies of different gases for compound $\{[Co(L-$

mal)(bpee)_{0.5}}]_n. Reproduced with permission from ref. 19i. Copyright© 2012, American Chemical Society.

An excellent example was shown by Rao *et al* where the incorporation of polar azo (–N=N–) group in pillar module of mixed ligand MOFs enhanced significantly the selectivity of CO₂ adsorption.¹⁹ⁱ They solvothermally prepared 3D homochiral MOFs based on the chiral L-malate dianion (L-mal) in combination with two different pyridyl-based linkers, {[M(L-mal)(azpy)_{0.5}]·2H₂O}_n and {[M(L-mal)(bpee)_{0.5}]·H₂O}_n (M = Co/Ni); [azpy = 4,4'-azobipyridine and bpee = 1,2-bis(4-pyridyl)ethylene] (Fig. 20a-b). All the frameworks are isostructural in which the chiral tridentate L-malate dianion bridges between the octahedral metal ions to form 2D layers of {M(L-mal)}_n that are separated (Fig. 20a), in a 3D porous framework, by azpy or bpee pillars (Fig. 20b). Gas adsorption studies on the dehydrated frameworks of {[Co(L-mal)(azpy)_{0.5}]·2H₂O}_n and {[Co(L-mal)(bpee)_{0.5}]·H₂O}_n show excellent selective CO₂ uptake over N₂, O₂, H₂, N₂ or Ar at 195 K. {[Co(L-mal)(azpy)_{0.5}]}_n displays higher CO₂ uptake (~22 wt %) compared to {[Co(L-mal)(bpee)_{0.5}]·H₂O}_n (~7 wt %) (Fig. 20c-d). The higher uptake of CO₂ in the dehydrated framework of {[Co(L-mal)(azpy)_{0.5}]}_n compared to {[Co(L-mal)(bpee)_{0.5}]}_n has been explained by the different polarity of the pore surfaces embedded in the pillar module, *i.e.* polar azo (–N=N–) group in azpy and ethylenic (–CH=CH–) group in bpee. This report indicates the simple way of increasing CO₂ uptake by increasing the polarity of the pore wall.

Two azo group (–N=N–) decorated mixed ligand based porous frameworks of Zn(II), {[Zn₂(μ₃-OH)(azbpy) (suc)_{1.5}]·(H₂O)₂}]_n and {[Zn(azbpy)_{0.5}(glut)(H₂O)]·(H₂O)}_n (azbpy = 4,4'-azobipyridine, suc = succinate dianion and glut = glutarate dianion) has been reported recently by our group that show selective CO₂ uptake (Fig. 21a-f).^{18d} In {[Zn₂(μ₃-OH)(azbpy) (suc)_{1.5}]·(H₂O)₂}]_n, tetranuclear zinc hydroxyl carboxylate SBU, {Zn₄(μ₃-OH)₂(COO)₆} is bridged by succinate dianions and azbpy linkers resulting a three dimensional (3D) coordination framework containing 1D channel along the crystallographic *a*-axis (Fig. 21a). The dimension of each channel is about 10.1×4.9 Å² and upon removal of the water molecules the framework shows about 24.1% void space (Fig. 21c). In case of {[Zn(azbpy)_{0.5}(glut)(H₂O)]·(H₂O)}_n the use of long chain glutarate results in a 1D ladder structure with lattice water molecules which were further locked by H-bonding to form a 2D supramolecular arrangement (Fig. 21b). In the crystal packing these 1D ladders are arranged in the crystallographic *a* axis to form a channel which is

occupied by lattice guest water molecules, and upon removal of the lattice water molecules the structure contains ~20.4% void space (Fig. 21d). The gas adsorption isotherms of desolvated forms of $\{[\text{Zn}_2(\mu_3\text{-OH})(\text{azbpy})(\text{suc})_{1.5}] \cdot (\text{H}_2\text{O})_2\}_n$ and $\{[\text{Zn}(\text{azbpy})_{0.5}(\text{glut})(\text{H}_2\text{O})] \cdot (\text{H}_2\text{O})\}_n$ shows selective adsorption of CO_2 over N_2 and shows a total CO_2 uptake of $54.45 \text{ cm}^3 \text{ g}^{-1}$ (Fig. 21e) and $66.84 \text{ cm}^3 \text{ g}^{-1}$ (Fig. 21f), respectively at 273 K and 1 atm pressure. This selective uptake of CO_2 is due to the presence of the $-\text{N}=\text{N}-$ group in the pore wall which can strongly interact with the quadrupole moment of CO_2 molecules.

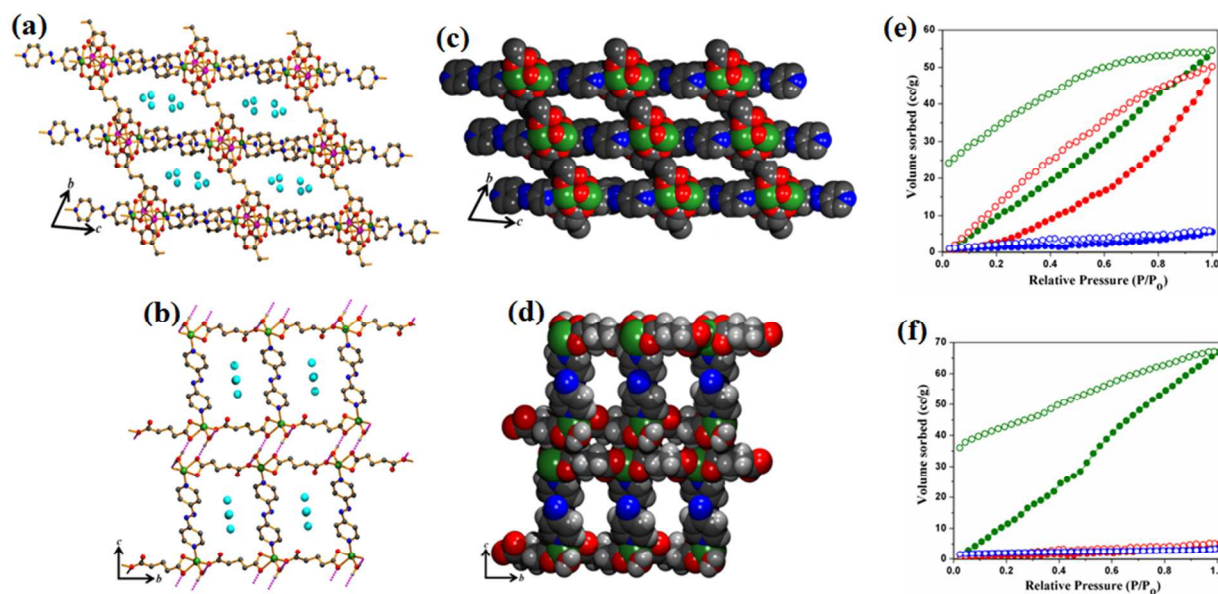


Fig. 21 (a) Three-dimensional structure of $\{[\text{Zn}_2(\mu_3\text{-OH})(\text{azbpy})(\text{suc})_{1.5}] \cdot (\text{H}_2\text{O})_2\}_n$ with water filled 1D channels; (b) view of the supramolecular 2D sheets in $\{[\text{Zn}(\text{azbpy})_{0.5}(\text{glut})(\text{H}_2\text{O})] \cdot (\text{H}_2\text{O})\}_n$ formed by H-bonding; (c) space-filling model without guest water molecules showing pores ($10.1 \times 4.9 \text{ \AA}^2$) along the a axis in $\{[\text{Zn}_2(\mu_3\text{-OH})(\text{azbpy})(\text{suc})_{1.5}] \cdot (\text{H}_2\text{O})_2\}_n$; (d) space-filling model without guest water molecules in $\{[\text{Zn}(\text{azbpy})_{0.5}(\text{glut})(\text{H}_2\text{O})] \cdot (\text{H}_2\text{O})\}_n$; (e, f) gas adsorption isotherms of $\{[\text{Zn}_2(\mu_3\text{-OH})(\text{azbpy})(\text{suc})_{1.5}] \cdot (\text{H}_2\text{O})_2\}_n$ and $\{[\text{Zn}(\text{azbpy})_{0.5}(\text{glut})(\text{H}_2\text{O})] \cdot (\text{H}_2\text{O})\}_n$, respectively CO_2 (green), H_2 (red) and N_2 (blue); filled and open circles represent adsorption and desorption, respectively. H_2 and N_2 adsorption isotherms were collected at 77 K and CO_2 adsorption isotherms of these compounds were collected at 273 K. Reproduced from ref. 18d.

A Cd(II)-based pillared-bilayer type framework $\{[\text{Cd}_4(\text{azpy})_2(\text{pyrdc})_4(\text{H}_2\text{O})_2] \cdot 9\text{H}_2\text{O}\}_n$ (azpy = 4,4'-azobipyridine and pyrdc = pyridine-2,3-dicarboxylate) has been synthesized by Maji *et al.*⁴¹ Each pyrdc ligand connects different Cd(II) centers in a unusual binding mode forming a 2D $[\text{Cd}_4(\text{pyrdc})_4]_n$ wavy sheet in the crystallographic *bc* plane (Fig. 22a). These sheets are then pillared by azpy in a criss-cross and canted fashion to form a pillared-bilayer network. Such arrangements of azpy results in convex type 1D channels along the crystallographic *c* axis with dimensions $3.5 \times 8.8 \text{ \AA}^2$ (Fig. 22a). The adjacent bilayers are connected to each other by hydrogen bonding interaction between guest water molecules in the interlayer spaces; the coordinated water molecule and oxygen of a carboxylate group of pyrdc resulting in a 3D supramolecular framework. Thus the overall framework possesses 1D channel in the intra-layer region and 2D space in the interlayer region. Due to the presence of $-\text{N}=\text{N}-$ group, the dehydrated framework shows very selective adsorption of CO_2 over Ar, CH_4 and H_2 at 195 K and the Langmuir surface area calculated from the CO_2 profile was found pretty high as $190 \text{ m}^2 \text{ g}^{-1}$ (Fig. 22b).

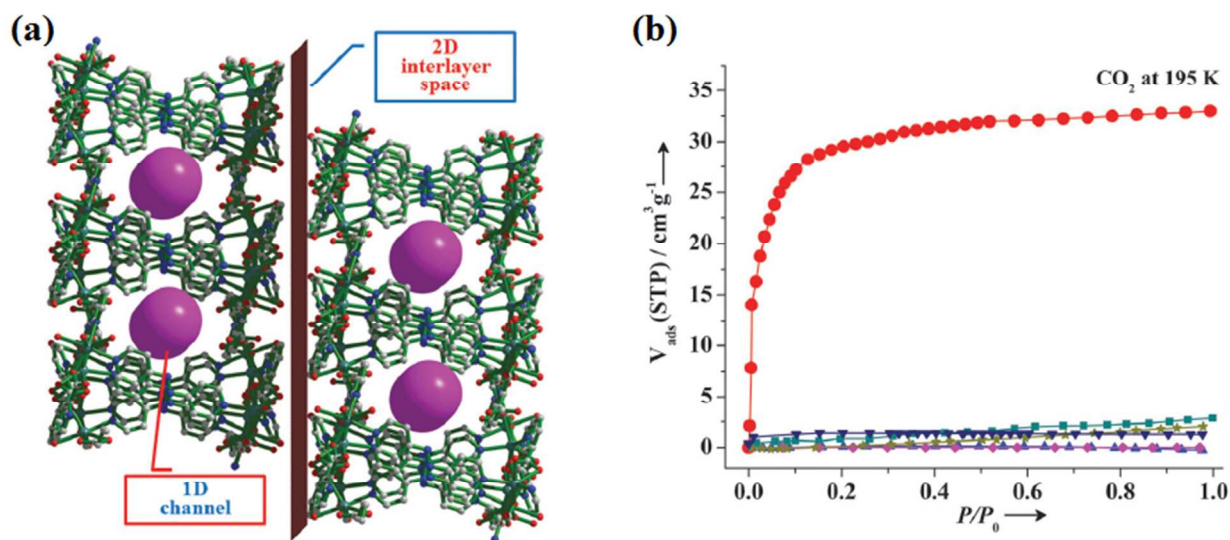


Fig. 22 (a) The pillared-bilayer 2D networks of $\{[\text{Cd}_4(\text{azpy})_2(\text{pyrdc})_4(\text{H}_2\text{O})_2] \cdot 9\text{H}_2\text{O}\}_n$ show 1D channels along the *c* axis and the 2D interlayer space in the *ab* plane, the latter separates the bilayers; (b) gas adsorption isotherms of $\{[\text{Cd}_4(\text{azpy})_2(\text{pyrdc})_4]\}_n$: CO_2 (circles), O_2 (squares), Ar (triangles), CH_4 (diamonds) at 195 K and H_2 (stars), N_2 (inverted triangles) at 77 K (P_0 is the saturated vapor pressure). Reproduced from ref. 41.

Along with azo based linkers, the azine variety has also been explored in latter stage for the same purpose of creating polar pore for selective CO₂ adsorption. In last few years our group has made significant contribution in synthesis of mixed ligand MOFs by using azine base linkers. A reversible single-crystal-to-single-crystal transformation of a 3D robust porous framework, and its dehydrated species made up with of Cu(II), a flexible dicarboxylate and an azine N,N'-donor ligand has been reported by our group.^{19j} The crystal structure of {[Cu(4-bpdb)_{0.5}(glut)](H₂O)₂}_n (4-bpdb = 1,4-bis-(4-pyridyl)-2,3-diaza-1,3-butadiene, glut = glutarate) revealed that each of paddle-wheel Cu₂(CO₂)₄ units are linked with glutarates to form a two-dimensional (2D) sheet which is pillared by an 4-bpdb linker in criss-crossed fashion, resulting in a honey comb like 3D framework of {[Cu(4-bpdb)_{0.5}(glut)](H₂O)₂}_n with 1D channel along the *c*-axis (Fig. 23a). The dimension of the channel is about 5.8 × 7.8 Å² and upon removal of the water molecules the framework contains about 34% void space. The dehydrated framework, {[Cu(azpy)_{0.5}(glut)]}_n selectively adsorbs CO₂ (6 wt%) over N₂ and the isosteric heat of adsorption for CO₂ is about 27 kJ/mol. The CO₂ selectivity and moderately high heat of adsorption of the dehydrated framework is attributed by the mutual interaction of quadruple moment CO₂ with the polar nature of azine (=N-N=) group in the pore surfaces (Fig. 23b). The dehydrated compound also displays step wise H₂O adsorption profile and MeOH, EtOH adsorption also supporting the polar nature of the pore.

In continuation of this work, we wanted to make some slide modification in the pore wall which can create some nice variation in the structure as well as in the adsorption properties. Here we have introduced methyl functionalized azine ligand 4-bpdh [4-bpdh = 2,5-bis-(4-pyridyl)-3,4-diaza-2,4-hexadiene], which will be polar as 4-bpdb but associated with bulky and hydrophobic methyl group.^{19k} The reaction of 4-bpdh with Cu(II) and glutarate dianion, ensuing in {[Cu(4-bpdh)_{0.5}(glut)](H₂O)₂}_n. Methyl functionalized framework has a similar structure to that of {[Cu(4-bpdb)_{0.5}(glut)](H₂O)₂}_n, only differing with respect to additional methyl groups pointing towards the channels and as a result channel dimension and void space of dehydrated framework has reduced (Fig. 23c). Like previous 4-bpdb containing compound, it also gives a reversible single-crystal-to-single crystal transformation between hydrated and dehydrated species. But surprisingly, compound with 4-bpdh shows a 50% enhancement in CO₂ adsorption (9 wt%) over {[Cu(4-bpdb)_{0.5}(glut)](H₂O)₂}_n which has been achieved by the pore wall modification by incorporating hydrophobic methyl groups, which is quite unprecedented. The isosteric heat of

adsorption for CO₂ of {[Cu(4-bpdh)_{0.5}(glut)](H₂O)}_n is 31.2 kJ/mol which is higher than non-methylated 4-bpdb containing framework (Fig. 23d). Water adsorption study also shows no uptake at low pressure ($P/P_0 \sim 0.4$) and after that a sharp rise was observed due to hydrophobic nature of the pore.

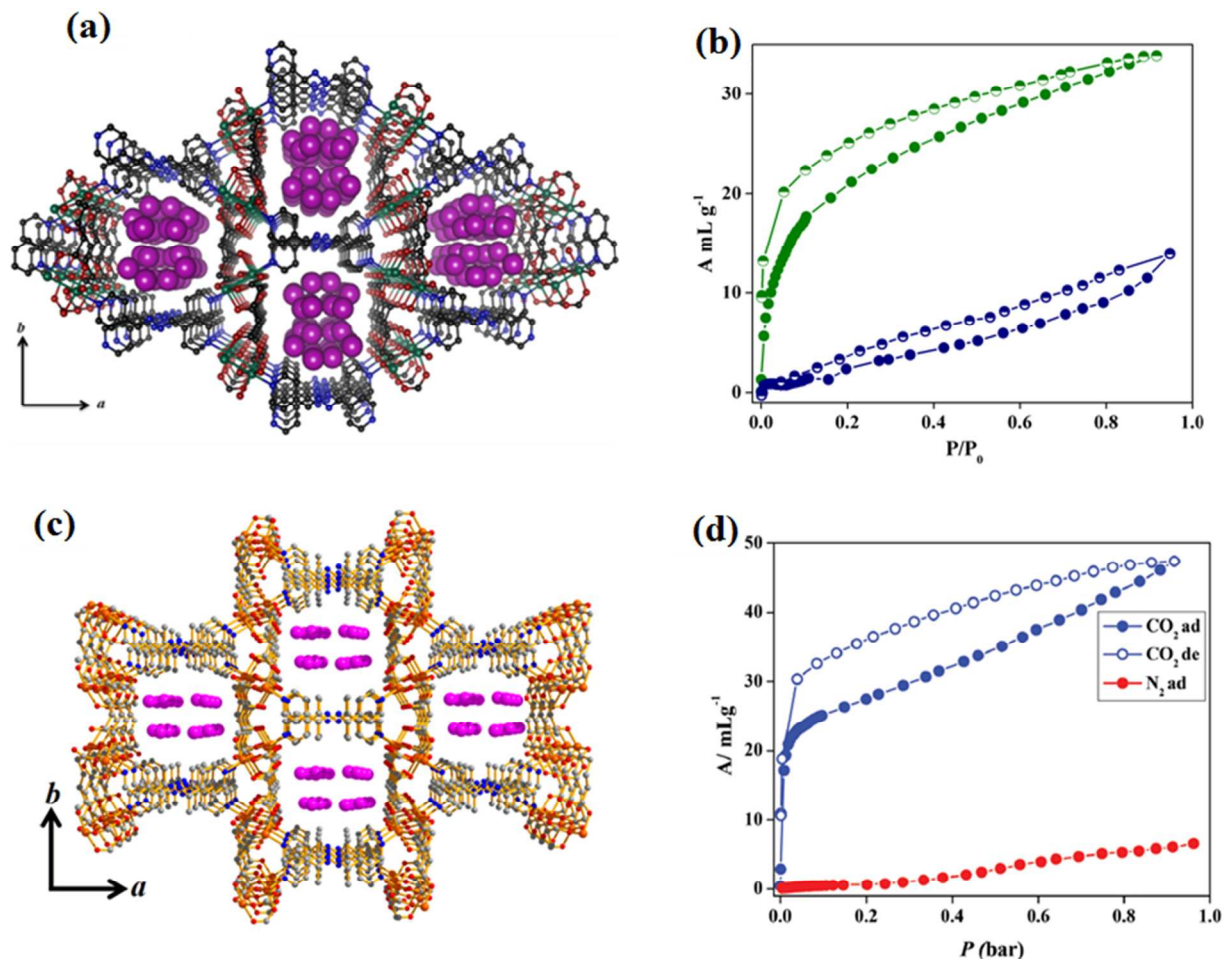


Fig. 23 (a) 3D honeycomb like structure of {[Cu(4-bpdb)(glut)](H₂O)₂}_n, with water molecules encapsulated in the nest of the honeycomb; (b) gas adsorption-desorption isotherms for {[Cu(4-bpdb)(glut)]_n}; CO₂ (green) at 195K; N₂ (blue) at 77K, adsorption: (filled shape), desorption: (half filled shape); (c) 3D honeycomb like structure of {[Cu(4-bpdh)(glut)](H₂O)}_n, with water molecules encapsulated in the nest of the honeycomb; (d) gas adsorption-desorption isotherms for {[Cu(4-bpdh)(glut)]_n}; CO₂ (green) at 195K; N₂ (blue) at 77K, adsorption: (filled shape), desorption: (half filled shape). (a & b) reproduced with permission from ref. 19j. Copyright© 2011, American Chemical Society; (c & d) reproduced from ref. 19k.

This example cited the role of hydrophobic group in the pore wall modification for the enhancement of CO₂ adsorption and evident the fact that in addition to the polar functionality, it is very essential to have some hydrophobic antenna on the pore wall of the MOFs, which can help to prevent the infiltration of water into the MOF. This type pore wall functionalization could be utilized for the development of MOFs with enhanced selective CO₂ sorption properties, having selectivity not only over N₂ but also over water.

Very recently, we have synthesized similar types of pillared-bilayer mixed ligand framework of Zn(II), {[Zn₂(NH₂-bdc)₂(4-bpdb)]·(H₂O)₄}_n and {[Zn₂(NH₂-bdc)₂(4-bpdh)]·(H₂O)₄}_n by using 5-amino-1,3-benzenedicarboxylate (NH₂-bdc) along with two different azine functionalized N,N'-donor linkers 4-bpdb and 4-bpdh (Fig. 24a-b). Here also in both compounds NH₂-bdc connects Zn(II) centers forming a 2D [Zn(NH₂-bdc)]_n sheet. The 2D sheets are joined by N,N'-linker to form a 2D pillared-bilayer framework and create 1D channels inside the bilayers. In the supramolecular structure, these 2D bilayers are further stitched by intermolecular hydrogen bonding and π-π interactions to generate a 3D supramolecular structure. The overall frameworks of both compounds do not possess two types of void space like the previously reported pillared-bilayer framework of Cd(II).¹⁹¹ The dimensions of the channel along the *b*-axis of {[Zn₂(NH₂-bdc)₂(4-bpdb)]·(H₂O)₄}_n is about 8.3 × 3.8 Å² (void space 27.1%) but in {[Zn₂(NH₂-bdc)₂(4-bpdh)]·(H₂O)₄}_n, the dimension of the channel reduces to 8.0 × 1.6 Å² (void space 17.1%) as the methyl groups of 4-bpdh are oriented within the pore. At 195 K both desolvated frameworks of {[Zn₂(NH₂-bdc)₂(4-bpdb)]·(H₂O)₄}_n and {[Zn₂(NH₂-bdc)₂(4-bpdh)]·(H₂O)₄}_n show selective type I CO₂ uptake profile and the uptake quantity are about 6.8 wt % (34.5 cm³ g⁻¹) and 3.6 wt % (18.3 cm³ g⁻¹), respectively (Fig. 24c). The difference between the CO₂ uptakes of {[Zn₂(NH₂-bdc)₂(4-bpdb)]·(H₂O)₄}_n and {[Zn₂(NH₂-bdc)₂(4-bpdh)]·(H₂O)₄}_n is well anticipated for larger pore size and higher solvent accessible void. The distinct hysteresis in CO₂ adsorption profile for {[Zn₂(NH₂-bdc)₂(4-bpdb)]·(H₂O)₄}_n can be explained in the light of strong interaction between quadruple moment of CO₂ and =N-N= group. Water adsorption study reveals that the desolvated forms of {[Zn₂(NH₂-bdc)₂(4-bpdb)]·(H₂O)₄}_n display extremely high water adsorption capacity even at low vapor pressure whereas desolvated forms of {[Zn₂(NH₂-bdc)₂(4-bpdh)]·(H₂O)₄}_n show very low water vapor uptake, which could be ascribed to the hydrophobic nature of the pore surface of {[Zn₂(NH₂-bdc)₂(4-bpdh)]·(H₂O)₄}_n (Fig. 24d).

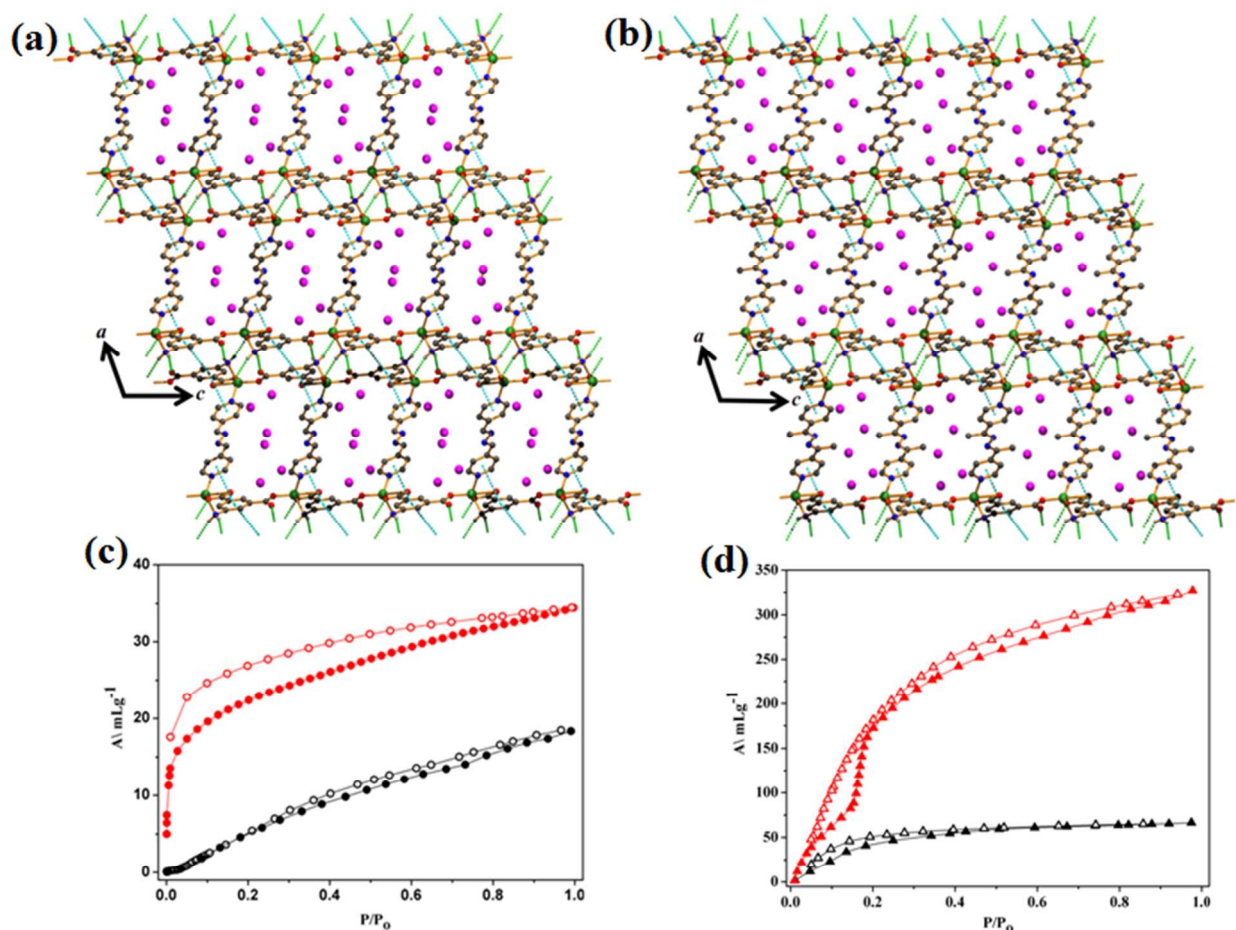


Fig. 24 (a, b) View of the 3D supramolecular framework structure of $\{[\text{Zn}_2(\text{NH}_2\text{-bdc})_2(4\text{-bpdb})]\cdot(\text{H}_2\text{O})_4\}_n$ and $\{[\text{Zn}_2(\text{NH}_2\text{-bdc})_2(4\text{-bpdh})]\cdot(\text{H}_2\text{O})_4\}_n$, respectively (π - π interactions: cyan dotted lines and H-bonding: green dotted lines) along b -axis; (c) CO_2 adsorption isotherms for $\{[\text{Zn}_2(\text{NH}_2\text{-bdc})_2(4\text{-bpdb})]\cdot(\text{H}_2\text{O})_4\}_n$ (red) and $\{[\text{Zn}_2(\text{NH}_2\text{-bdc})_2(4\text{-bpdh})]\cdot(\text{H}_2\text{O})_4\}_n$ (black) at 195 K: adsorption (filled circles), desorption (open circles); (d) water-vapor adsorption isotherms of $\{[\text{Zn}_2(\text{NH}_2\text{-bdc})_2(4\text{-bpdb})]\cdot(\text{H}_2\text{O})_4\}_n$ (red) and $\{[\text{Zn}_2(\text{NH}_2\text{-bdc})_2(4\text{-bpdh})]\cdot(\text{H}_2\text{O})_4\}_n$ (black) at 298 K: adsorption (filled triangles), desorption (open triangles). Reproduced from ref. 191.

Morsali *et al* prepared two azine functionalized three-dimensional porous Zn(II) MOFs, $[\text{Zn}_2(\text{oba})_2(4\text{-bpdb})]\cdot(\text{DMF})_x$ and $[\text{Zn}_2(\text{oba})_2(4\text{-bpdh})]\cdot(\text{DMF})_y$ through mechanochemistry, by using 4,4'-oxybisbenzoic acid (H_2oba) and the same linear N,N'-donor ligands 4-bpdb and 4-bpdh (Fig. 25a-d).⁴² In both the cases oba connects to Zn(II) centers forming two-dimensional (2D) metal carboxylate layers and these 2D layers pillared by N,N'-donor ligands forming 3D framework structure. The use of nonfunctionalized (4-bpdb) and methyl-functionalized (4-bpdh)

N,N'-donor ligands has led to the construction of frameworks with different topologies and metal–ligand connectivity and therefore different pore sizes and accessible voids (Fig. 25a-d).

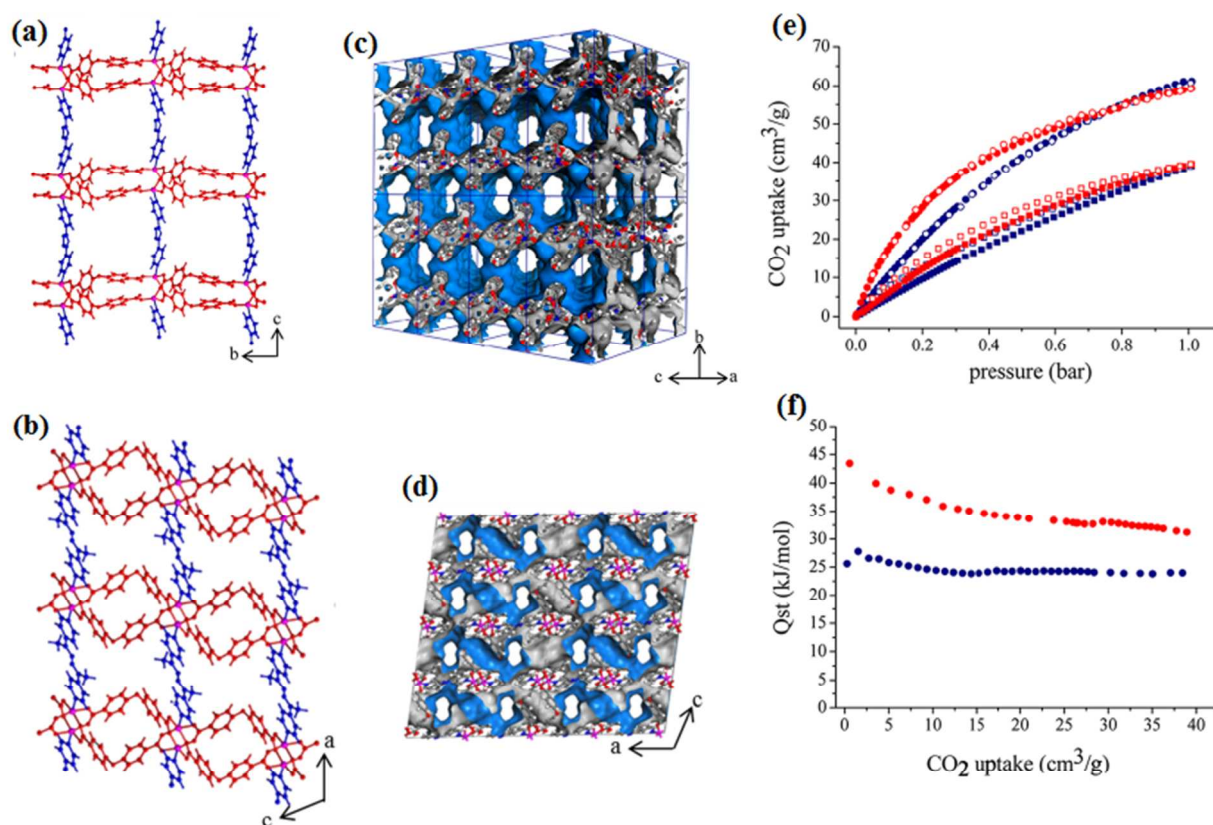


Fig. 25 (a) Layers of Zn(II)-oba (in red) pillared by 4-bpdb (in blue) in $[\text{Zn}_2(\text{oba})_2(4\text{-bpdb})]\cdot(\text{DMF})_x$; (b) layers of Zn(II)-oba (in red) pillared by 4-bpdh (in blue) in $[\text{Zn}_2(\text{oba})_2(4\text{-bpdh})]\cdot(\text{DMF})_y$; (c, d) 3D Connolly surface representation of porous $[\text{Zn}_2(\text{oba})_2(4\text{-bpdb})]\cdot(\text{DMF})_x$ and $[\text{Zn}_2(\text{oba})_2(4\text{-bpdh})]\cdot(\text{DMF})_y$, respectively; (e) CO₂ isotherms collected at 273 and 298 K of $[\text{Zn}_2(\text{oba})_2(4\text{-bpdb})]\cdot(\text{DMF})_x$ (blue) and $[\text{Zn}_2(\text{oba})_2(4\text{-bpdh})]\cdot(\text{DMF})_y$ (red); (f) isosteric heat of adsorption (Q_{st}) for CO₂ at different CO₂ loadings of $[\text{Zn}_2(\text{oba})_2(4\text{-bpdb})]\cdot(\text{DMF})_x$ (blue) and $[\text{Zn}_2(\text{oba})_2(4\text{-bpdh})]\cdot(\text{DMF})_y$ (red). Reproduced with permission from ref. 42. Copyright © 2014, American Chemical Society.

Both the frameworks demonstrate azine functionalized 1D solvent filled channels but $[\text{Zn}_2(\text{oba})_2(4\text{-bpdh})]\cdot(\text{DMF})_y$ ($5.6 \times 3.8 \text{ \AA}^2$) (Fig. 25c) has narrower pore channels than $[\text{Zn}_2(\text{oba})_2(4\text{-bpdb})]\cdot(\text{DMF})_x$ ($6.8 \times 7.8 \text{ \AA}^2$) (Fig. 25d). Desolvated forms of these two frameworks display relatively high CO₂ uptake capacities at 273 and 298 K temperature over N₂

(Fig. 25e) with high heat of adsorption (Fig. 25f). The relatively high heat of adsorption value of both the frameworks has been attributed to the strong interaction between CO₂ and azine functional group of frameworks.

Conclusion

It is evident from the overall discussion that the mixed ligand MOFs with different carboxylate ligands and N,N'-donor linkers; shows a meaningful advantage, particularly for the separation of carbon dioxide from gas mixture due to the balancing presence of their stability and ease of their design. The interactions between the porous MOFs and gas molecules are mainly van der Waals type which can be augmented by the increase of pore size in MOFs. Thus along with the suitable pore size it is also necessary to incorporate some specific sites, such as open metal sites, different functional groups and/or hetero atoms on the pore surface to enhance their strong interactions with CO₂ molecules. The cooperative utilization of such factors in the design of MOF can effectively produce some material which may be useful for high CO₂ storage and separation of CO₂ from mixture of gases at moderate temperatures. In this connection it is ascertained that the mixed ligand MOF have enormous prospect for the design of such materials that can show selective CO₂ adsorption. Different successful strategies to construct porous mixed ligand MOFs with functional sites for selective CO₂ adsorption have been briefly discussed in this highlight and for better understanding of the context we have divided our exploration into three parts. Firstly, we have described the strategy of improving the CO₂ adsorption by controlling the pore size using N,N'-donor ligands of variable lengths. In the following part, we have discussed how CO₂ adsorption can be amplified in presence of coordinatively unsaturated metal sites and subsequently we have highlighted the rate of enhancement of CO₂ adsorption by modifying the organic ligands with different polar functional groups like -F, -NH₂, -CONH-, -N=N-, =N-N=.

The above three criteria are important for the design of the porous mixed ligand MOFs having capability of selective CO₂ adsorption. Thus it can be achieved by careful inclusion of these major criteria individually or mutually. The careful exploration in this way may result some fruitful materials which can show more selective adsorption of CO₂ over N₂ having viability in industrial separation of CO₂, and we believe that the mixed ligand MOF will be the key player to accomplish such revolutionary target.

References

- 1 (a) R. Quadrelli and S. Peterson, *Energy Policy*, 2007, **35**, 5938; (b) K. S. Lackner, S. Brennan, J. M. Matter, A.-H. A. Park, A. Wright and B. van der Zwaan, *Proc. Natl. Acad. Sci. U. S. A.*, 2012, **109(33)**, 13156.
- 2 (a) R. A. Feely, S. C. Doney and S. R. Cooley, *Oceanography*, 2009, **47**, 22; (b) M. Z. Jacobson, *Energy Environ. Sci.*, 2009, **2**, 148; (c) S. Solomon, G.-K. Plattner, R. Knutti and P. Friedlingstein, *Proc. Natl. Acad. Sci. U. S. A.*, 2009, **106(6)**, 1704; (d) M. R. Allen, D. J. Frame, C. Huntingford, C. D. Jones, J. A. Lowe, M. Meinshausen and N. Meinshausen, *Nature*, 2009, **458**, 1163.
- 3 (a) R. S. Haszeldine, *Science*, 2009, **325**, 1644; (b) J. T. Yeh, K. P. Resnik, K. Rygle and H. W. Pennline, *Fuel Process. Technol.*, 2005, **86**, 1533.
- 4 (a) K. T. Chue, J. N. Kim, Y. J. Yoo, S. H. Cho and R. T. Yang, *Ind. Eng. Chem. Res.*, 1995, **34**, 591; (b) J. Zhang, P. A. Webley and P. Xiao, *Energ. Convers. Manage*, 2008, **49**, 346; (c) E. Díaz, E. Muñoz, A. Vega and S. Ordóñez, *Chemosphere*, 2008, **70**, 1375.
- 5 (a) H. Li, M. Eddaoudi, M. O'Keffee and O. M. Yaghi, *Nature*, 1999, **402**, 276; (b) S. Kitagawa, S.-I. Noro, R. Kitaura, *Angew. Chem. Int. Ed.*, 2004, **43**, 2334; (c) R. Haldar, R. Matsuda, S. Kitagawa, S. J. George and T. K. Maji, *Angew. Chem. Int. Ed.*, 2014, **53**, 11772; (d) J. F. Van Humbeck, T. M. McDonald, X. Jing, B. M. Wiers, G. Zhu and J. R. Long, *J. Am. Chem. Soc.*, 2014, **136**, 2432.
- 6 (a) S. Yuan, W. Lu, Y.-P. Chen, Q. Zhang, T.-F. Liu, D. Feng, X. Wang, J. Qin and H.-C. Zhou, *J. Am. Chem. Soc.*, 2015, **137**, 3177; (b) Y.-B. Zhang, H. Furukawa, N. Ko, W. Nie, H. J. Park, S. Okajima, K. E. Cordova, H. Deng, J. Kim and O. M. Yaghi, *J. Am. Chem. Soc.*, 2015, **137**, 2641; (c) R. Singh and P. K. Bharadwaj, *Cryst. Growth Des.*, 2013, **13**, 3722.
- 7 (a) N. R. Champness, *Dalton Trans.*, 2006, 877; (b) J. Heo, Y.-M. Jeon and C. A. Mirkin, *J. Am. Chem. Soc.*, 2007, **129**, 7712; (c) S.-M. Fang, Q. Zhang, M. Hu, E. C. Sañudo, M. Du and C.-S. Liu, *Inorg. Chem.*, 2010, **49**, 9617; (d) Q. Zhang, J. Zhang, Q.-Y. Yu, M. Pan and C.-Y. Su, *Cryst. Growth Des.*, 2010, **10**, 4076.
- 8 (a) J. A. Mason, M. Veenstra and J. R. Long, *Chem. Sci.*, 2014, **5**, 32; (b) F. Gándara, H. Furukawa, S. Lee and O. M. Yaghi, *J. Am. Chem. Soc.*, 2014, **136**, 5271; (c) L. J. Murray, M. Dincă and J. R. Long, *Chem. Soc. Rev.*, 2009, **38**, 1294; (d) S. Ma and H.-C. Zhou, *Chem. Commun.*, 2010, **46**, 44.

- 9 (a) J.-R. Li, R. J. Kuppler and H.-C. Zhou, *Chem. Soc. Rev.*, 2009, **38**, 1477; (b) S. Qiu, M. Xue and G. Zhu, *Chem. Soc. Rev.*, 2014, **43**, 6116; (c) T. Rodenas, I. Luz, G. Prieto, B. Seoane, H. Miro, A. Corma, F. Kapteijn, F. X. Llabrés i Xamena and J. Gascon, *Nat. Mater.*, 2015, **14**, 48.
- 10 (a) B. Gole, A. K. Bar, A. Mallick, R. Banerjee and P. S. Mukherjee, *Chem. Commun.*, 2013, **49**, 7439; (b) M. Zhao, S. Ou and C.-D. Wu, *Acc. Chem. Res.*, 2014, **47**, 1199; (c) R. K. Das, A. Aijaz, M. K. Sharma, P. Lama and P. K. Bharadwaj, *Chem. Eur. J.*, 2012, **18**, 6866.
- 11 (a) S. Sen, N. N. Nair, T. Yamada, H. Kitagawa and P. K. Bharadwaj, *J. Am. Chem. Soc.*, 2012, **134**, 19432; (b) T. Panda, T. Kundu and R. Banerjee, *Chem. Commun.*, 2013, **49**, 6197; (c) T. Yamada, K. Otsubo, R. Makiurac and H. Kitagawa, *Chem. Soc. Rev.*, 2013, **42**, 6655.
- 12 (a) F. Gándara, F. J. Uribe-Romo, D. K. Britt, H. Furukawa, L. Lei, R. Cheng, X. Duan, M. O’Keeffe and O. M. Yaghi, *Chem. Eur. J.*, 2012, **18**, 10595; (b) M. G. Campbell, D. Sheberla, S. F. Liu, T. M. Swager and M. Dincă, *Angew. Chem. Int. Ed.*, 2015, **54**, 4349. (c) B. Bhattacharya, A. Layek, Md. M. Alam, D. K. Maity, S. Chakrabarti, P. P. Ray and D. Ghoshal, *Chem. Commun.*, 2014, **50**, 7858.
- 13 (a) A. Mallick, B. Garai, M. A. Addicoat, P. St. Petkov, T. Heine and R. Banerjee, *Chem. Sci.*, 2015, **6**, 1420; (b) B. Gole, A. K. Bar and P. S. Mukherjee, *Chem. Commun.*, 2011, **47**, 12137; (c) G. J. Halder, C. J. Kepert, B. Moubaraki, K. S. Murray and J. D. Cashion, *Science*, 2002, **298**, 1762.
- 14 (a) H. Furukawa, N. Ko, Y. B. Go, N. Aratani, S. B. Choi, E. Choi, A. Ö. Yazaydin, R. Q. Snurr, M. O’Keeffe, J. Kim, O. M. Yaghi, *Science*, 2010, **329**, 424; (b) O. K. Farha, A. Ö. Yazaydin, I. Eryazici, C. D. Malliakas, B. G. Hauser, M. G. Kanatzidis, S. T. Nguyen, R. Q. Snurr and J. T. Hupp, *Nature Chemistry*, 2010, **2**, 944.
- 15 (a) K. Sumida, D. L. Rogow, J. A. Mason, T. M. McDonald, E. D. Bloch, Z. R. Herm, T.-H. Bae and J. R. Long, *Chem. Rev.*, 2012, **112**, 724; (b) J. Liu, P. K. Thallapally, B. P. McGrail, D. R. Brown and J. Liu, *Chem. Soc. Rev.*, 2013, **42**, 6655; (c) S. Chaemchuen, N. A. Kabir, K. Zhou and F. Verpoort, *Chem. Soc. Rev.*, 2013, **42**, 9304; (d) J.-R. Li, Y. Ma, M. C. McCarthy, J. Sculleya, J. Yub, H.-K. Jeongb, P. B. Balbuenab and H.-C. Zhou, *Coord. Chem. Rev.*, 2011, **255**, 1791.
- 16 (a) M. C. Das, S. Xiang, Z. Zhang and B. Chen, *Angew. Chem. Int. Ed.*, 2011, **50**, 10510; (b) M. Du, C.-P. Li, C.-S. Liu and S.-M. Fang, *Coord. Chem. Rev.*, 2013, **257**, 1282.

17 (a) H. Chun, D. N. Dybtsev, H. Kim and K. Kim, *Chem. Eur. J.*, 2005, **11**, 3521; (b) T. K. Maji, R. Matsuda and S. Kitagawa, *Nat. Mater.*, 2007, **6**, 142; (c) P. Manna, B. K. Tripuramallu and S. K. Das, *Cryst. Growth Des.*, 2014, **14**, 278.

18 (a) P. Kanoo, R. Matsuda, M. Higuchi, S. Kitagawa and T. K. Maji, *Chem. Mater.*, 2009, **21**, 5860; (b) Z. Zhang, J. Liu, Z. Li and J. Li, *Dalton Trans.*, 2012, **41**, 4232; (c) Y. Hijikata, S. Horike, M. Sugimoto, M. Inukai, T. Fukushima and S. Kitagawa, *Inorg. Chem.*, 2013, **52**, 3634; (d) B.-Q. Ma, K. L. Mulfort and J. T. Hupp, *Inorg. Chem.*, 2005, **44**, 4912; (e) B. Bhattacharya, D. K. Maity, R. Dey and D. Ghoshal, *CrystEngComm*, 2014, **16**, 4783.

19 (a) S. Couck, J. F. M. Denayer, G. V. Baron, T. Remy, J. Gascon and F. Kapteijn, *J. Am. Chem. Soc.*, 2009, **131**, 6326; (b) X. Gu, Z.-H. Lu and Q. Xu, *Chem. Commun.*, 2010, **46**, 7400; (c) Z. Chen, S. C. Xiang, H. D. Arman, P. Li, D. Y. Zhao and B. Chen, *Eur. J. Inorg. Chem.*, 2010, 3745; (d) J. L. C. Rowsell and O. M. Yaghi, *J. Am. Chem. Soc.*, 2006, **128**, 1304; (e) P. Pachfule, Y. Chen, J. Jiang and R. Banerjee, *Chem. Eur. J.*, 2012, **18**, 688; (f) Y. Zhao, H. Wu, T. J. Emge, Q. Gong, N. Nijem, Y. J. Chabal, L. Kong, D. C. Langreth, H. Liu, H. Zeng and Jing Li, *Chem. Eur. J.*, 2011, **17**, 5101; (g) S. Parshamoni, S. Sanda, H. S. Jena and S. Konar, *Chem. Asian J.*, 2015, **10**, 653; (h) Z.-H. Xuan, D.-S. Zhang, Z. Chang, T.-L. Hu and X.-H. Bu, *Inorg. Chem.*, 2014, **53**, 8985; (i) C. M. Nagaraja, R. Haldar, T. K. Maji and C. N. R. Rao, *Cryst. Growth Des.*, 2012, **12**, 975; (j) R. Dey, R. Haldar, T. K. Maji, and D. Ghoshal, *Cryst. Growth Des.*, 2011, **11**, 3905; (k) B. Bhattacharya, R. Haldar, R. Dey, T. K. Maji and D. Ghoshal, *Dalton Trans.*, 2014, **43**, 2272; (l) B. Bhattacharya, R. Haldar, D. K. Maity, T. K. Maji and D. Ghoshal, *CrystEngComm*, 2015, **17**, 3471.

20 B. Chen, S. Ma, F. Zapata, F. R. Fronczek, E. B. Lobkovsky, and H.-C. Zhou, *Inorg. Chem.*, 2007, **46**, 1233-1236.

21 S. D. Burd, S. Ma, J. A. Perman, B. J. Sikora, R. Q. Snurr, P. K. Thallapally, J. Tian, L. Wojtas, and M. J. Zaworotko, *J. Am. Chem. Soc.*, 2012, **134**, 3663.

22 P. Nugent, Y. Belmabkhout, S. D. Burd, A. J. Cairns, R. Luebke, K. Forrest, T. Pham, S. Ma, B. Space, L. Wojtas, M. Eddaoudi and M. J. Zaworotko, *Nature*, 2013, **495**, 80.

23 T. Panda, P. Pachfule and R. Banerjee, *Chem. Commun.*, 2011, **47**, 7674.

24 B. Bhattacharya, R. Dey, P. Pachfule, R. Banerjee and D. Ghoshal, *Cryst. Growth Des.*, 2013, **13**, 731.

- 25 (a) Y.-S. Bae, O. K. Farha, A. M. Spokoyny, C. A. Mirkin, J. T. Hupp and R. Q. Snurr, *Chem. Commun.*, 2008, 4135; (b) B. L. Chen, N.W. Ockwig, A. R. Millward, D. S. Contreras and O. M. Yaghi, *Angew. Chem. Int. Ed.*, 2005, **44**, 4745; (c) M. Dinca, A. Dailly, Y. Liu, C. M. Brown, D. A. Neumann and J. R. Long, *J. Am. Chem. Soc.*, 2006, **128**, 16876; (d) O. K. Farha, A. M. Spokoyny, K. L. Mulfort, M. F. Hawthorne, C. A. Mirkin, J. T. Hupp, *J. Am. Chem. Soc.*, 2007, **129**, 12680.
- 26 H. Sakamoto, R. Matsuda, S. Bureekaew, D. Tanaka, and S. Kitagawa, *Chem. Eur. J.*, 2009, **15**, 4985.
- 27 Z. Zhang, S. Xiang, K. Hong, M. C. Das, H. D. Arman, M. Garcia, J. U. Mondal, K. M. Thomas and B. Chen, *Inorg. Chem.*, 2012, **51**, 4947.
- 28 P. Kanoo, A. C. Ghosh, S. T. Cyriac, and T. K. Maji, *Chem. Eur. J.*, 2012, **18**, 237.
- 29 S. Horike, R. Matsuda, D. Tanaka, M. Mizuno, K. Endo and S. Kitagawa, *J. Am. Chem. Soc.*, 2006, **128**, 4222.
- 30 Y.-S. Bae, B. G. Hauser, O. K. Farha, J. T. Hupp, R. Q. Snurr, *Microporous Mesoporous Mater.*, 2011, **141**, 231.
- 31 C. F. Leong, T. B. Faust, P. Turner, P. M. Usov, C. J. Kepert, R. Babarao, A. W. Thornton and D. M. D'Alessandro, *Dalton Trans.*, 2013, **42**, 9831.
- 32 (a) P. Chowdhury, C. Bikkina and S. Gumma, *J. Phys. Chem. C*, 2009, **113**, 6616; (b) R. L. Amey, *J. Phys. Chem.*, 1974, **78**, 1968
- 33 (a) M. Kandiah, M. H. Nilsen, S. Usseglio, S. Jakobsen, U. Olsbye, M. Tilset, C. Larabi, E. A. Quadrelli, F. Bonino and K. P. Lillerud, *Chem. Mater.*, 2010, **22**, 6632; (b) M. L. Foo, S. Horike, T. Fukushima, Y. Hijikata, Y. Kubota, M. Takata and S. Kitagawa, *Dalton Trans.*, 2012, **41**, 13791; (c) P. Pachfule, Y. Chen, J. Jiang and R. Banerjee, *J. Mater. Chem.*, 2011, **21**, 17737.
- 34 A. Santra, I. Senkovska, S. Kaskel and P. K. Bharadwaj, *Inorg. Chem.*, 2013, **52**, 7358.
- 35 D. S. Zhang, Z. Chang, Y. F. Li, Z. Y. Jiang, Z. H. Xuan, Y. H. Zhang, J. R. Li, Q. Chen, T. L. Hu and X. H. Bu, *Sci. Rep.*, 2013, **3**, 3312.
- 36 (a) R. Vaidhyanathan, S. S. Iremonger, K. W. Dawson and G. K. H. Shimizu, *Chem. Commun.*, 2009, 5230; (b) R. Vaidhyanathan, S. S. Iremonger, G. K. H. Shimizu, P. G. Boyd, S. Alavi, T. K. Woo, *Science*, 2010, **330**, 650.
- 37 Q.-G. Zhai, Q. Lin, T. Wu, L. Wang, S.-T. Zheng, X. Bu and P. Feng, *Chem. Mater.*, 2012, **24**, 2624.

- 38 R. Haldar, S. K. Reddy, V. M. Suresh, S. Mohapatra, S. Balasubramanian and T. K. Maji, *Chem. Eur. J.*, 2014, **20**, 4347.
- 39 C.-H. Lee, H.-Y. Huang, Y.-H. Liu, T.-T. Luo, G.-H. Lee, S.-M. Peng, J.-C. Jiang, I. Chao, and K.-L. Lu, *Inorg. Chem.*, 2013, **52**, 3962.
- 40 B. Liu, D.-S. Li, L. Hou, G.-Ping Y., Y.-Y. Wang and Q.-Z. Shia, *Dalton Trans.*, 2013, **42**, 9822.
- 41 P. Kanoo, G. Mostafa, R. Matsuda, S. Kitagawa and T. K. Maji, *Chem. Commun.*, 2011, **47**, 8106.
- 42 M. Y. Masoomi, K. C. Stylianou, A. Morsali, P. Retailleau and D. Maspoch, *Cryst. Growth Des.*, 2014, **14**, 2092.

For Table of Content use

Selective carbon dioxide adsorption by mixed ligand porous coordination polymers

Biswajit Bhattacharya and Debajyoti Ghoshal^{†*}

Department of Chemistry, Jadavpur University, Kolkata, 700 032, India

